UNIVERSITÀ DEGLI STUDI DI MILANO

PhD in Epidemiology, Environment and Public Health XXXIII cycle

Department of Clinical Sciences and Community Health

PhD Research Thesis

Air pollution exposure in pregnancy: nasal microbiota and extracellular vesicle communication as potential mechanism to explain adverse birth outcomes

MED/44-Occupational Medicine

Dott. Jacopo Mariani (matr. N° R11864)

Supervisor: Prof.ssa Angela Cecilia Pesatori

PhD coordinator: Prof. Carlo La Vecchia

A.A. 2019-2020

SUMMARY

ABSTRACT

BACKGROUND: Particulate matter (PM) exposure has been linked to the exacerbation of respiratory and cardiovascular conditions as well as to adverse effects on fetal growth. To link the cross-talk that might occur between respiratory system and placenta after PM exposure, it has been proposed a novel mechanism of cell to cell communication mediated by extracellular vesicles (EVs). EVs are involved in both biological and pathological processes including pregnancy state. As PM interacts firstly with the nares, bacterial nasal microbiota (bNM) is one of the first compartments hit by PM exposure. This interaction might lead to structural and functional modifications within the bNM, which could cause variations within the EVs signaling network, which might lead to an improper immune response to PM stimuli.

AIM: The main aim of the project was to identify how PM exposure might modify the homeostasis and composition of whole EV signaling network and bNM and the leading to a possible impact on newborn development.

Subject recruitment*:* 518 volunteer pregnant women were enrolled during the 11th week of pregnancy at the 'Clinica Mangiagalli'-Fondazione IRCCS Ca' Granda – Ospedale Maggiore Policlinico, Milan, Italy. Among them, a group of subjects composed by 65 pregnant women, who agreed to participate to a more complex study protocol, was also identified.

Exposure assessment, EV and Microbiota measurement:

Exposure to PM concentrations was assessed using data obtained from FARM models for the whole population. In addition, individual exposure to short-term PM levels was retrieved through a personal sampler worn by the subgroup of 65 pregnant women. Plasmatic concentration and cellular origin of EVs were characterized by Nanoparticle tracking analysis (NTA) and flow cytometry, respectively. We investigated the bNM structure and characteristics of 65 pregnant women both at the enrolment (T0) and the following Monday

during the cardiovascular screening (T1) through metabarcoding analysis of the V3–V4 regions of the 16s rRNA gene.

Statistical analysis:

Multivariable linear regression models were applied to test the associations between PM exposure (retrieved from both FARM models and personal sampler) and the majority of the collected outcomes such as maternal, foetal/newborns, and cardiovascular parameters as well as for bNM data.

On the other hand, to evaluate possible associations between PM concentrations and EV characteristics negative binomial regression models for count data with over-dispersion were performed.

In addition, multiple comparison method based on Benjamini-Hochberg False Discovery Rate (FDR) were applied for high number of comparisons.

RESULTS

In the whole population, PM_{10} exposure (measured at different time windows) resulted in decreased release of total amount of EVs, with the strongest effect related to concentration measured 13 weeks before the enrolment (13wks), whereas an inverse tendency was observed for exposure to $PM_{2.5}$, although these associations were not significant. More reliable data on the finest fractions (PM_1, $PM_{2.5}$ and PM_4) are given by personal sampler worn by a subgroup of women for a very short time period preceding the blood drawing (1.5 hours). As we considered this extremely acute effect, we observed a generalized increment in the EV count. Noteworthy, among the different analyzed EV subtypes, the levels of HERV-w+ EVs were the only to be increased by each tested PM_{10} time-lag. The same models applied on bNM data showed a reductions in terms of diversity (Shannon/Faith_pd ratio) and relative abundance of the genera *Corynebacterium spp.* and *Staphylococcus spp.* In addition, when the possible role of bNM as effect modifier between PM exposure and EVs

release was investigated, we observed for the pregnant women with a balanced bNM an increment in terms of circulating EVs after daily PM stimuli.

Moreover, increments of the heart rate values were observed after exposure to both PM_{10} and $PM_{2.5}$ levels measured the day before the cardiovascular screening (Day -1).

Focusing on newborn's outcomes, decrements of the gestational age at birth were associated to PM concentrations measured throughout the gestation or during the 2nd trimester.

CONCLUSIONS: To our knowledge, this is the first exploring the role of bNM and the EV cross-talk in determining the effects of PM exposure levels on healthy pregnancies as well as on newborn outcomes. The results obtained so far might suggest a possible role exerted by both EV concentration and the bNM in pregnant women in mediating the effects of PM exposure.

INTRODUCTION

Environmental exposure to air pollutants, including particulate matter (PM), has been linked to the exacerbation of several respiratory and cardiovascular conditions in both adults and children [1]. In addition, PM exposure has been also observed to heighten the risk associated with adverse pregnancy outcomes such as, gestational diabetes mellitus, preterm delivery, still-birth, hypertensive disorders in pregnancy (HDP), low birthweight (LBW), and small for gestational ages (SGA) infants [2,3]. Occurring in almost 10% of pregnancies mostly as gestational hypertension or preeclampsia, HDP have been related to increased maternal and neonatal morbidity and mortality [4]. It has been also observed that HDP can lead through growth and development impairments of the intrauterine fetus to premature birth, death, and LBW infants [3]. More common in developing countries than in developed ones, LBW has been associated with both health and development impairment in children, but also with adverse health outcomes in later life [5]. On the other hand, SGA is referred to those fetuses or newborns whose birthweight is below the 10^{th} percentile at a specified gestational age and gender [6]. Interestingly, several studies have shed light on the possible role played by both PM and air pollutant exposure in triggering the risk of LBW infant delivering, especially taking into account the first three months of pregnancy, which has considered fundamental for a correct fetus development during later stages [7]. Although the underlying mechanism responsible for the development of adverse birth outcomes due to PM exposure is still largely unknown, it has been documented the ability of PM to reach the systemic circulation and trigger local inflammatory reaction [8].

Recently, the extracellular vesicle (EV) release has been proposed as a cell to cell communication mechanism, which might explain the possible cross-talk between respiratory system and placenta as well as the systemic effects triggered by PM exposure [9,10]. EVs are extracellular structures, delimited by a lipid bilayer and released by different cellular

types into biological fluids, representing a powerful and not yet fully understood mode of communication [11]. Acting as carriers of several biological mediators, such as DNA, RNA, non-coding RNA, protein and other soluble factors, EVs are involved in numerous biological and pathological processes, including cancer, metabolic diseases, atherosclerosis, development of Chronic Obstructive Pulmonary Disease (COPD) and allergic airway inflammation [12–14]. Moreover, it is well known that EVs could play a fundamental role during pregnancy: syncytiotrophoblast-derived EVs, indeed, are released in increased amount during pathological pregnancy [15,16]. In particular, these EVs derived from placenta syncytial epithelium, are recognized and internalized by monocytes enhancing their pro-inflammatory activity leading to modification of the maternal environment [17].

When entering the upper airways, PM firstly interacts with the nasal mucosa and also with the bacterial nasal microbiota (bNM), which is defined as the clustered microorganism community referred only to the bacteria population, inhabiting several regions of the human body and linked to fundamental biological functions provided to the host [18]. Characterized by specific bacteria structure and connections in the different body districts, the microbiota is dynamic and sensible to the effects of drugs, antibiotics, lifestyle and environmental factors [19]. These stressor factors, including air pollution and PM exposure, can lead to a structural modification of the indigenous bacterial community, called dysbiosis, which can potentially cease and/or modify the biological function provided by the microbiota [19]. In particular, the negative effects of PM exposure on nasal bacteria community, associated with a reduction of bacterial diversity and relative abundance of bacterial strains has been identified [20]. This effect has been also observed in peculiar pathological airways conditions, such as cystic fibrosis and chronic rhinosinusitis [21,22]. Interestingly, it was recently reported that an unbalanced bNM, characterized by an over-abundance of

Moraxella spp. can be considered as an effective modifier of the association between PM exposures and EV release modifications [23].

Considering the evidence linking air pollution exposure to adverse conditions including pregnancy adverse outcomes, the main aim of the present project is to identify how PM exposure, here chosen as paradigmatic environmental stressor, might modify both the extracellular vesicle (EV) signaling network and the maternal nasal bacterial composition, leading to an alteration of the host physiological homeostasis and eventually impacting on maternal health and newborns development.

THE PREGNANCY STATE: main characteristics and related physiological changes in a normal pregnancy

The term pregnancy describes the period in which a fetus develops inside a woman's uterus after conception. Usually, a normal human gestation lasts about 40 weeks, which can be grouped into three stages: the first trimester (from 0 to 13th weeks), the second trimester (from 14th to 27th weeks) and the third trimester (from 27th to 40th weeks), the last characterized by the delivery process. A pregnancy is defined "full term" if delivery occurs between the 39th and 41st weeks of gestation whereas childbirths taking place before the 37th are defined as pre-term, those after the 42nd as post-term, those between the 37th and 39th weeks are defined as early- term, and those born between the 41st and 42nd weeks as late-term (Figure 1).

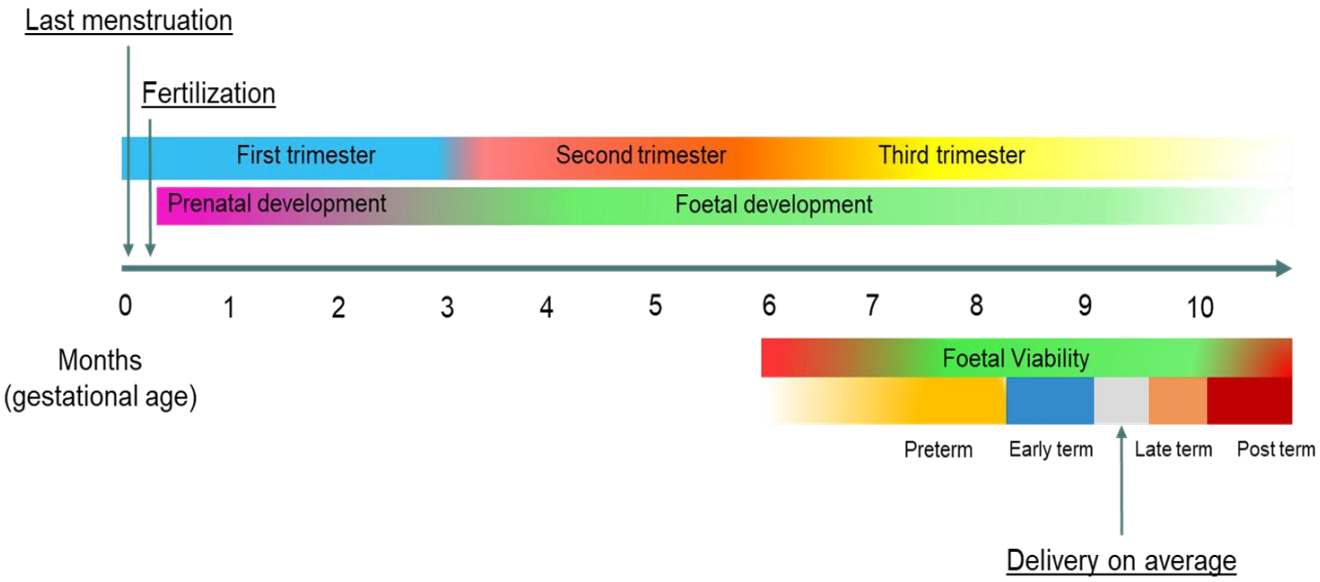

Figure 1. Timeline of pregnancy, including from top to bottom: Trimesters, embryo/fetus development, gestational age in months, viability and maturity stages. For reference see [24]

Throughout the gestational period, high-quality prenatal care is often provided to pregnant women to improve the chance of carrying out a proper gestation and having a healthy infant. Prenatal care can include a different variety of procedures such maternal clinical history-

taking, medical prophylaxis, and advising as well as both maternal and fetal screening [25]. During maternal and fetal assessment, different parameters can be inspected to get an overview of the conditions of both fetal and maternal states and some parameters, out of the most screened ones, are listed and described in Table 1.

Table 1. List of the most common maternal and fetal parameters screened during the gestation

Prenatal care observed parameters	Clinical relevance
Maternal parameters	
Pregnancy-associated plasma protein A (PAPPA)	Low levels have been linked to Cornelia De Lange Syndrome, Threatened Abortion, Pregnancy loss, Intrauterine fetal demise, SGA, preeclampsia [26]
human chorionic gonadotropin (hCG)	Levels at or above the discriminatory zone could indicate pregnancy complications. Typically paired with ultrasound evaluation to improve sensitivity and specificity [27]
Fetal parameters	
Crown-rump length	Estimation of gestational age [28]
Nuchal translucency thickness	Increasing values are commonly related to phenotypic expression of chromosomal abnormalities [29]
Fetal heart rate	Severe variations have been linked to fetal adverse outcomes [30]
Ductus venous pulsatility index (DVPI)	Critical values denote many fetal conditions that can give rise to cardiovascular complications [31]
Uterine artery pulsatility index (UtaPI)	Potential marker to predict pregnancy adverse outcomes linked to utero-placental insufficiency before the onset of clinical features [32]
Blood pressure	Marker to monitor in clinical settings such as preeclampsia and gestational hypertension [33]

The first few weeks after conception are generally considered the most important pregnancy stage, characterized by placentation, a crucial process necessary for a proper prenatal and fetal development [34,35]. This process begins when the blastocyst, constituted by an inner cell mass surrounded by a layer of mononucleotide trophoblast, adheres to the wall of the decidual uterine endometrium. Through several processes of cellular differentiation, the trophoblast layer generates the largest parts of the placenta and fetal membranes, whereas the inner cell mass directly generates the embryo and umbilical cord as well as the placental mesenchyme. These changes give rise to the proper placenta structure, a circular discoidal organ with a diameter of circa 22 cm and an approximate weight of 470 g aimed to facilitate the uptake of nutrients and oxygen from maternal blood and characterized by a constant vascular network development throughout the pregnancy to further improve the exchange efficiency as fetal demand arises [35]

In addition, along with placentation, pregnant women undergo to significant anatomical and physiological changes mainly involving the cardiovascular, metabolic, endocrine and respiratory systems throughout the gestational period in order to achieve a proper fetal development [36]. Cardiovascular changes in pregnancy occur since the earliest phase and consist mostly in a progressive increment of plasma volume and cardiac output characterized by a peripheral vasodilation throughout the gestational period as well as a decrement of blood pressure values in the first and second trimesters. In addition, it has been observed increased levels of fibrinogen and VII, IX, X clotting factors generating a hyper-coagulable state to set up the homeostasis after delivery, however predisposing also the pregnant women to the risk of venous thrombosis.

To allow fetal growth, modifications within the maternal metabolism occur, including the increase of changes in the intestinal intake of amino acids and calcium as well as the serum levels of cholesterol and triglycerides. Variations in the glucose metabolism are observed, resulting in an increased glycogen storage and glucose peripheral use to promote fetal

development while maintaining adequate maternal nutrition [36,37]. Considering the endocrinal modifications, the modifications of several hormone concentrations are observed in the whole gestational period to compensate the anatomical changes and the fetal demands. For example, the first trimester of gestation is characterized by an increased amount of released insulin along with a higher sensitivity to the pancreatic hormone, which guides progressively in the further trimesters to a maternal insulin resistance [36].

Focusing on the respiratory system, a significant increase in oxygen demand during normal pregnancy due to an increase in the metabolic rate and consumption of oxygen is compensated by an increment in tidal volume, causing a 40–50% increase in minute ventilation, which define the volume of inhaled or exhaled air from a person's lungs per minute. Anatomically, the respiratory system undergoes to an extension of the dead volume of lungs due to relaxation of muscles together with a reduction of the total pulmonary capacity by diaphragmatic excursion which in turns is compensate by an increased chest circumference [37].

In addition, to allow the establishment, maintenance, and completion of a healthy pregnancy, changes in both adaptive and innate immune responses occur. Indeed, to avoid fetal rejection, it has been observed that macrophages along with regulatory T cells play a pivotal role in establishing a self-tolerant maternal environment to prevent a triggered immune responses [38].

Due to the wide range of anatomical and physiological changes that the human body undergoes to carry out a proper gestation, several adverse outcomes have been related to pregnancy marking it as critical period. Therefore, pregnant women have been also observed to be more sensitive to the negative effects of environmental toxicants, including air pollution, which are known to heighten the already existent risk to develop gestational related complications [39].

PARTICULATE MATTER: Characteristics and effects on human health

Exposure to air pollutants has been widely studied as a major health global risk and the consequences associated to it are numerous and observed at each stage of life [1]. Each year, air pollution concentrations are linked globally to millions of deaths occurring as a consequence of the damages principally induced on both the respiratory and the cardiovascular systems [1]. Among them, in the 2018 it was observed that 5.25 % of all deaths were attributable to ambient particulate matter (PM) exposure, becoming the 8^{th} leading risk for deaths, with a total of 2.94 million deaths globally [40]. Emitted by anthropic and natural sources, PM consists in a mixture of air-transported particles constantly varying in terms of chemical composition, according to the season time and the geographical localization [1]. Indeed, it has been identified that PM is composed by both solid and liquid particles including nitrates, sulphate, elemental and organic carbon, organic polycyclic aromatic hydrocarbons, metal ions, and biological compounds such as microorganism cell fragments [41]. Composition and toxicity of this complex mixture depend on the source it originates from [42]. Considering urban PM, the major reported sources are vehicular emissions and industrial biomass burning, accounting for the 25% and 15% of total global contributions, respectively [8]. Beside the outdoor sources, it has been observed that PM generated by domestic activities could sometimes exceed the particle concentration levels detected in the outdoor environment [1]. Commonly, PM particles are separated in two size-based categories: particulate matter (PM_{10}) with aerodynamic diameter equal or less than 10 μm and fine particulate matter ($PM_{2.5}$) with an aerodynamic diameter of less than 2.5 μm [43] which are able to travel through the respiratory system, penetrate down to the alveoli and to disseminate itself into the circulation [1,8].

The principal health risks determined by PM exposure can be mainly linked to the induced oxidative stress promoting cellular inflammation and both mutagenicity and genotoxicity,

respectively [8,44,45]. Oxidative stress effects induced by PM particles leads to inflammatory reaction and cytotoxicity through the production of free radicals such as reactive oxygen species (ROS). Conversely, induced genetic changes are related to the presence of inorganic and aromatic organic components, with the organic part accounting for the 75% of the total DNA damages.-are [8,45].

Epidemiological studies have reported an association between both short and long term exposure to PM and increased mortality, involving different organs or system as shown in Fig 2 [1,8,46].

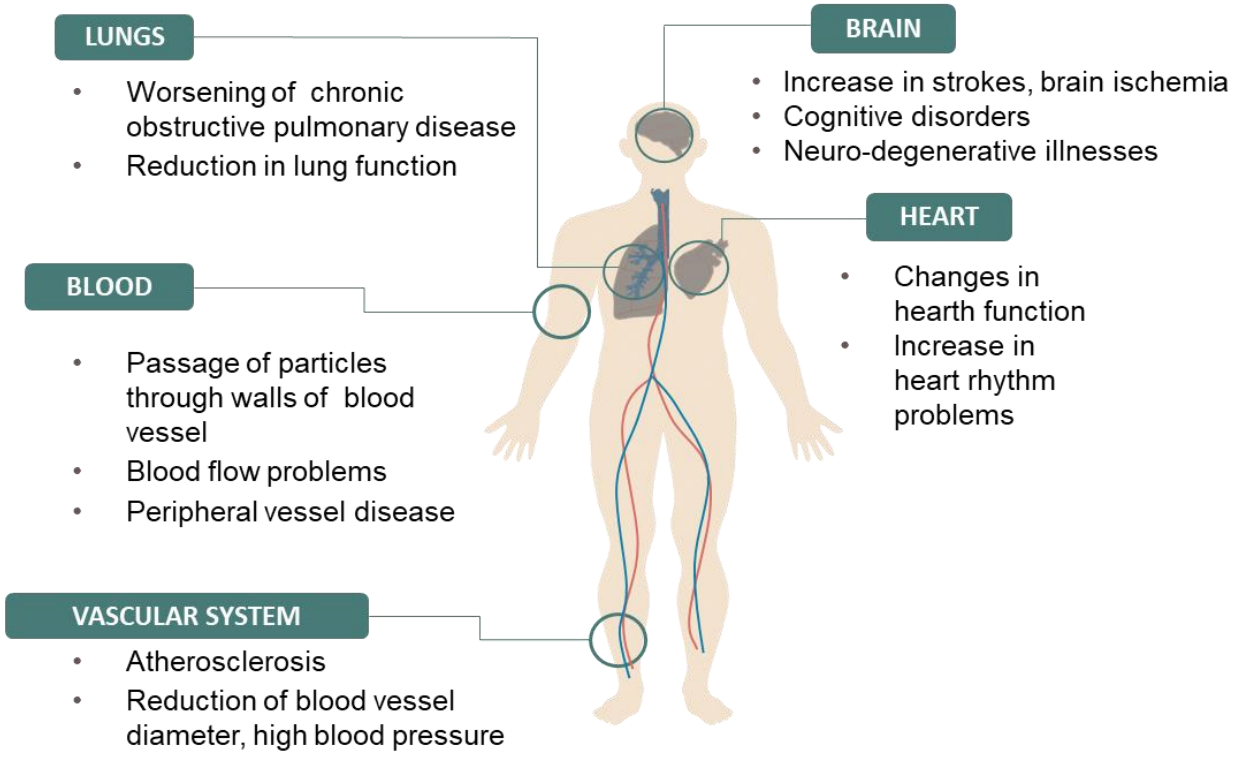

Figure 2. Summary of the adverse air pollution and particulate matter effects on human health

PM effects on cardiovascular system have been also observed in pregnant women, which can be considered a susceptible population [47]. For example, it was reported that PM_{10} levels during the whole pregnancy are associated with an increase systolic blood pressure (SBP), and each 10 g/m^3 increment is associated with an increased risk of pregnancy-induced hypertension [48]. Hypertension is often linked to a decreased heart rate (HR)

variability , which is defined as the cyclical changes of sinus rhythm, a well-defined indicator of cardiac autonomic function also associated with PM effects [8,49]. In particular, blood pressure (BP) decreases during the first trimester of pregnancy by 5-10 mmHg reaching its lowest point by mid-pregnancy, as a compensatory increase in blood volume and vasodilatation occurs. Gestational hypertension is defined when either two separate BP measurements are greater than or equal to 140mmHg systolic or 90mmHg diastolic compared to previously collected normal blood pressure values or an acute value of SBP greater than 160mmHg or diastolic blood pressure (DBP) greater than 110mmHg occur [50].

PARTICULATE MATTER: air particulate particles effects on newborn outcomes.

In addition to the cardiovascular effects, different associations of trimester-specific PM levels have been found with pregnancy complications, such as preeclampsia, gestational diabetes mellitus, preterm delivery, still-birth, LBW SGA), as shown in Figure 3 [7,8,39,51,52].

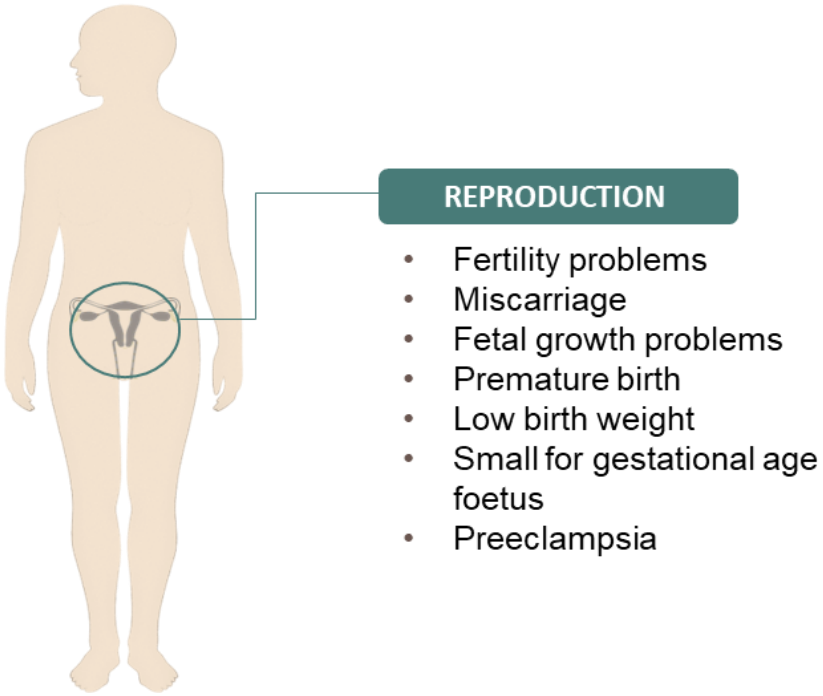

Figure 3. Summary of the known PM exposure related complications of during gestation

The World Health Organization (WHO) defines LBW as an infant weighing at birth less than 2.500g. On the other hand, SGA is defined as infants weighing less than the 10th percentile at a specified gestational age as well as neonate whose birth weight is at least 2 standard deviations (-2 SD) below the mean for the gestational age [6]. SGA definition is not straightforward as for LBW requiring information about gestational age, measurement of birth weight, head circumference and a reference data from a relevant and comparable population [53]. Both LBW and SGA have been linked to trigger the risk of adverse outcomes in both the later stage of life and adulthood, including asthma, low Intelligence Quotient (IQ),

atopic dermatitis [5], ischemic heart disease, chronic hypertension [54], and insulin resistance/metabolic syndrome [53] as well as motor and cognitive impairments [55]. Interestingly, maternal $PM_{2.5}$ exposure was negatively correlated with the weight at birth and the strongest correlation was observed with the exposures experienced during the first trimester [7,56]. On the other hand, maternal $PM_{2.5}$ exposure levels during the whole pregnancy are found to positively correlate with the risk for a fetus SGA, observing an increased risk for each 10 $\mu g/m^3$ increment in $PM_{2.5}$ concentration [7,57]. In agreement with the above reported evidences, Hannam et al. [58] and Symanski et al. [59] reported a higher risk of SGA linked with $PM_{2.5}$ exposure during the second and third-trimester as well as through the whole pregnancy. In addition, consistent effects were also identified for PM_{10} exposure on both LBW and SGA outcomes [60].

Nevertheless the associations identified between different PM fraction levels and both LBW and SGA are rather consistent [52,61], only a small part of the inhaled particles reach and accumulate themselves in organs other than lungs system, indeed unidentified biological mechanisms may exist to explain the PM effects on both the reproductive system and the developing fetus [61], as well as on the other organs [9].

EXTRACELLULAR VESICLES: A possible biomarker to investigate systemic particulate matter effects

In the last decade, extracellular vesicles (EVs) have been proposed as suitable mediators of PM effects on human health. Indeed, they might be released in response to PM exposure and influence adverse peripheral outcomes, particularly by being involved in the underlying PM toxicity mechanisms as well as by their ability to translocate from the pulmonary capillary bed through the systemic circulation, reach and connect distant organs, and release their transported bioactive molecules into the target cells finally inducing biological changes [9,10].

EVs are biological structures delimited by a lipid bilayer, released by any human cells into biological fluids in a different manner depending on the physiological state, able to be bind recipient cell membranes and finally release their biological active cargoes [11].

Generally stratified by their size into microvesicles (MVs) (100-1000 nm diameter range) and exosomes (40-100 nm diameter range), these kinds of EVs are also characterized by a different biogenesis, which in both case involve membrane-traffic processes. The formers originate by an outward budding at cell surface whereas exosomes are generated within the endosomal system as intraluminal vesicles (ILVs) and secreted during the fusion of multi-vesicular bodies (MVBs) with the inner cell membrane as summarized in Figure 4 [62].

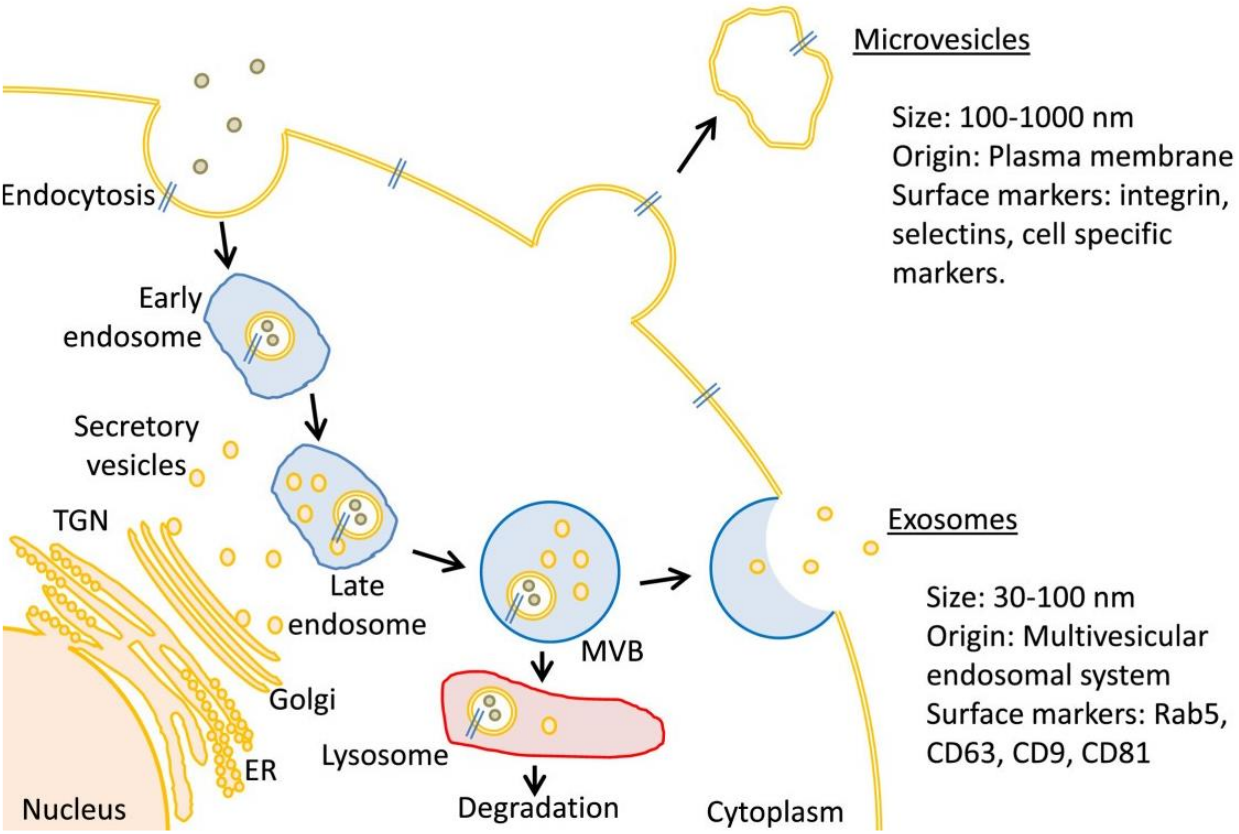

Figure 4. Microvesicles (MVs) and exosomes biogenesis. MVs arise from budding of the plasma membrane. Exosomes originate from the endosomal trafficking system and, therefore, are more regular in shape and size. ER: endoplasmic reticulum; miRNA: microRNA; TGN: trans-Golgi network; MVB: multi-vesicular bodies. For reference see [63].

Upon released in the extracellular space, both MVs and exosomes have to reach and deliver their content to the recipient cells in order to enable functional response. This communication mechanism involve docking at plasma membrane followed by specific membrane receptor bindings, which promote either vesicles internalization or their fusion with target cell surface. Determined by specific interactions between proteins at EV surface, which usually define vesicle cellular origin, and receptors localized at the recipient cell plasma membrane, the EV binding to their target cells is characterized by cellular-specificity as observed in the liver, lungs and neurons as well as in dendritic cells [11,64]. Once bound,

EVs induce a functional response on recipient cells both by protein-receptor binding and transported biomolecules released into the cytoplasm of target cells.

Initially described as a means of eliminating unneeded compounds from the cellular environment, EVs can carry a variety of biological molecules, including microRNA (miRNA), messenger RNA (mRNA), DNA, lipids, and proteins either activating or modifying various processes in the recipient cells after internalization [10,11]. Moreover, as both the released number of vesicles and the cargo composition can vary depending on the physio-pathological state, EVs have been also investigated as a biomarker of the development and progression of adverse conditions [65]. Therefore, variations in the total concentration of specific EVs and cargo modifications from a physiological pattern have been observed in certain forms of CVD [66,67], in neurodegenerative disease such as in the early progression of Alzheimer's diseases, during infectious diseases, diabetes, cancer and pulmonary diseases [10].

To support the choice of EVs as a suitable mediator of PM effects spread throughout the body sites, both *in vitro* and human studies showed a relationship between PM levels and EV modifications in terms of concentration and carried molecules [9,10]. Considering the *in vitro* studies, different cellular lines like human macrophages, THP-1, BEAS-2 and A549 showed modifications induced by different PM fractions, particularly characterized by an increment of the amount of released EVs [68–71]. Consistently, also the data derived from human studies confirmed the effects of PM exposure in modifying the amount and the content of circulating vesicles. For example, different inhaled particle levels were associated with an alteration in the amount of produced endothelial EVs in overweight subjects [72] as well as in diabetic patients showing also an increased procoagulant potential of MV fraction, might worsening the pro-thrombotic risk linked to air pollution exposure [73].

PM variations on EVs were also identified in terms of their cargo modifications. The screening of miRNA encapsulated into EVs pointed out that PM exposure was associated

to the upregulation of miR-128 and miR-302c levels, involved in coronary artery disease and cardiac hypertrophy and heart failure pathways respectively [71]. Moreover, it was suggested that EVs released after PM_{10} exposure may promote both blood coagulation and an increased risk of CVD events via their RNA cargo, particularly due to the downregulation of five miRNAs (hsa-let-7c-5p, hsa-miR-331-3p, hsa-miR-185-5p, hsa-miR-106a-5p, hsa-miR-652-3p) [74].

Merging the abovementioned considerations, EVs result as an interesting biomarker to inspect alterations induced by air pollution as well as to predict the development of unhealthy states including those observed during gestation as released-vesicles can take part to both normal and disease-related pregnancy processes [15].

EXTRACELLULAR VESICLES: normal and pathological pregnancy from an EV point of view

Since the interest in studying EVs vesicles as suitable biomarker of diverse physiological and pathological processes has been increased and established, their activity and characteristics have been also investigated in a wide range of healthy and adverse conditions, including gestation [15].

During pregnancy a wide amount of EVs are observed into maternal circulation, playing important role as modulator in a variety of processes like implantation, migration and invasion of trophoblast, and cellular adaptation to physiological changes (Figure 5) [75,76]. Embryo implantation is an early and essential step for successful pregnancy where the embryo reaches the endometrial surface of the uterus and invades the maternal epithelium and circulation to form the placenta. At this stage, it has been observed that EVs can mediate the fetal-maternal cross-talk highlighting the potential role of transported miRNA [77,78]. Exosomial-miR-30d was observed to be transferred from the endometrial epithelium to

embryo-trophectoderm, improving the adhering ability of the embryo during implantation as well as to positively regulate the expression of Itgb3, Itga7 and Cdh5 genes, involved in embryo adhesion [79]. Recent evidences have underlined a link between EVs and immunomodulation during pregnancy, a delicate equilibrium by which the maternal immune system both tolerates the growing fetus and preserves its normal activities to prevent uterine infections [80]. It has been observed that placenta derived EVs enriched on their surface by syncytin-1 protein, which is encoded by human endogenous retrovirus group W (HERV-w) envelope gene, could participate in the establishment of an immune-tolerant microenvironment interacting with specific maternal cells, might through the immunosuppressive domain in the syncytin-1 protein structure [81,82]. EVs carrying HERV-w proteins could also take part in the mechanism underlying the appropriate nutrient and gaseous supply to the fetus, mediating the maternal-fetal cross-talk binding themselves to the receptor of endothelial and cyto-trophoblast cells [82].

Noteworthy, *in vitro* studies have highlighted that exosomes derived from maternal tissues could take part to spiral artery remodeling and cardiovascular adaptations, mandatory to meet the maternal and fetal metabolic demands especially in the early stages of pregnancy [83,84]. Moreover, due to both the proinflammatory activity and the increased possibility to reach gestational tissue at term labor, recent studies pointed out that exosomes could been reasonably involved into the birth timing by increasing the uterine inflammation to prepare the uterus for delivery [85].

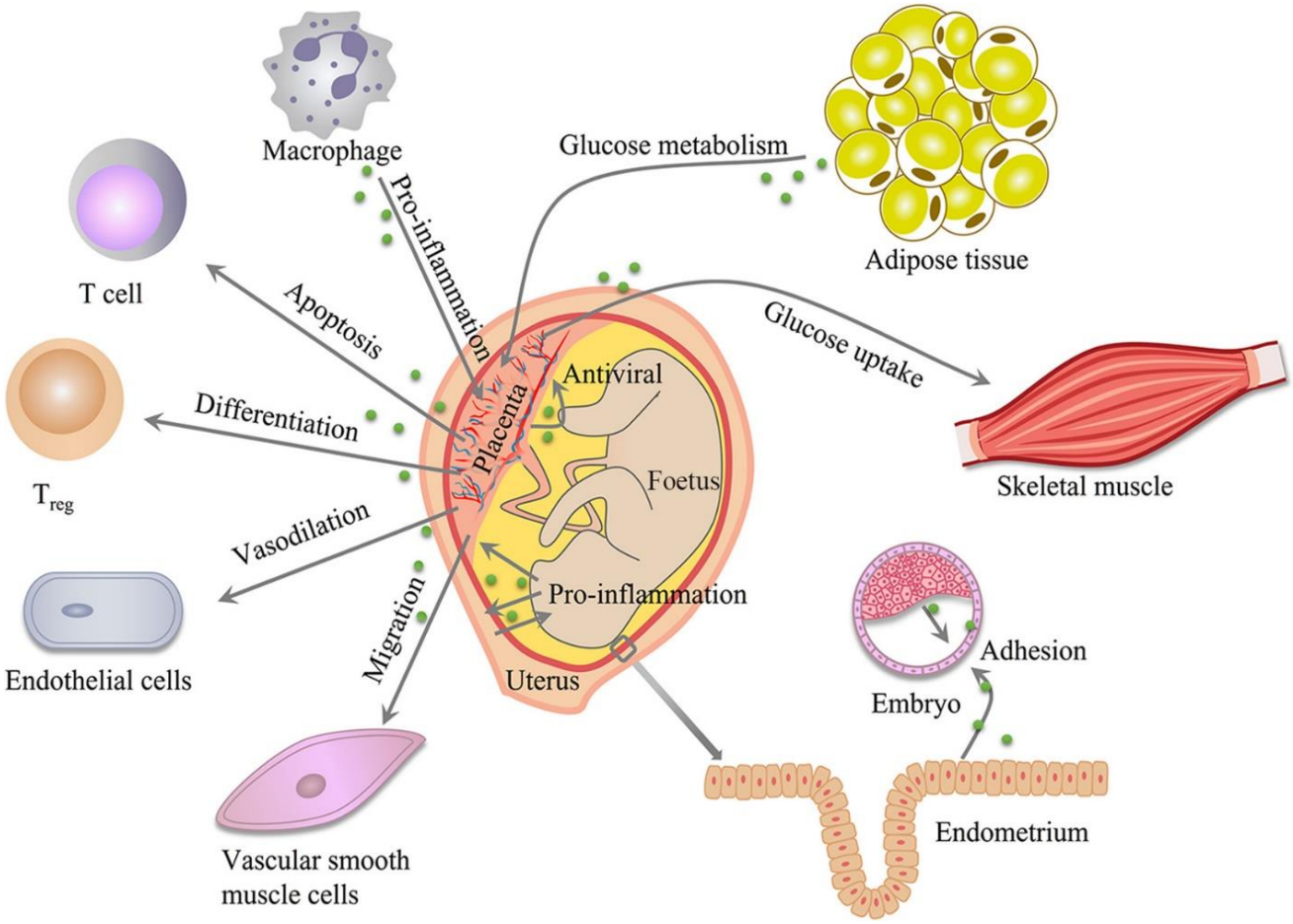

Figure 5. Effects of EVs in normal pregnancy can mediate fetal-maternal communications contributing to embryo implantation by promoting trophoblast adhesion. Placenta can interact with immune cells via EVs to regulate maternal tolerogenicity across the gestation. EVs can activate endothelial cell (ECs) and vascular smooth muscle cells (VSMCs) as well as accelerate glucose metabolism in the placenta and skeletal muscle. Moreover, inflammation signals of maturation in EVs can prepare uterus for delivery. For references see [15].

EV concentration levels, composition, and bioactivity changes are involved in pregnancy-related diseases such as pre-eclampsia (PE), gestational diabetes and other pregnancy outcomes [15]. In patients with PE, different concentrations of plasmatic placenta-derived exosomes during the early and late stages of disease have been observed [86]. Moreover, several variations in terms of different encapsulated miRNAs were reported, among which authors suggest miR-486-1-5p and miR-486-2-5p as candidate indicators of early stage PE [87]. Noteworthy, fluctuations in EV concentrations derived from the syncytiotrophoblast layer, a multinucleate interface between the maternal and fetal environments with

fundamental roles throughout the pregnancy, were implicated in PE pathophysiology [88]. In particular, both Vargas et al. [82] and Levine et al. [88] have reported that the concentrations of syncytin-1 EVs were lowered in PE patients when compared to healthy pregnant women. Studies conducted to identify the role of EVs in gestational diabetes showed a possible diagnostic value of placenta-derived exosomes as their concentration is significantly greater in mothers with gestational diabetes compared with normal pregnancies [89].

Interestingly, it has been observed that the amount of placental-derived EVs positively correlate with the weight at birth, suggesting a ~14% higher levels in normal fetus compared to SGA cases [90]. Moreover, during the second trimester of gestation higher expression levels of miR-20b-5p, miR-942-5p, miR-324-3p, miR-223-5p and miR-127-3p were linked to the likelihood to have SGA infants in later stages [91].

THE NASAL & UPPER RESPIRATORY TRACT MICROBIOTA: a possible actor in the respiratory homeostasis

The upper respiratory tract (UTR) is constantly exposed to biological and chemical particulates, shaping and characterizing the environment of the sinuses, nasopharynx, oropharynx and nasal cavity [92]. In particular, the nasal cavity firstly interacts with air pollutants, fungal spores, allergens and microbes deriving from the external environment, which activate the host immunity and the nasal epithelium [21]. Inhabiting the epithelium of the nares by niche-specific microorganisms, the involvement of the bacterial nasal microbiota (bNM) and the whole UTR microbiota in different physiological and pathological processes has been recently reported, as an association between microbiota composition and the onset and progression of adverse conditions [19].

Generally composed by both resident and transient microbes, the bNM is characterized by the presence of commensals and pathobionts which constitute the three most observed phyla: Actinobacteria, Firmicutes and Proteobacteria [21]. Many studies focused their effort in identifying the bNM composition and observed that the three above described phyla are largely represented by, *Corynebacterium spp., Staphylococcus spp., Cutibacterium spp., Streptococcus spp., Dolosigranulum spp., and Moraxella spp.* genera respectively [19,20].

The bNM is not a static compartment but its composition is plastic and can vary over different seasons (winter vs summer) and life-stages, as showed in Figure 6 [21]. Considering the bNM of infants, a shift in composition is observed occurring in the first two years of life hence a bacterial community resembling more the skin or vaginal maternal microbiota is switched with one dominated by *Dolosigranulum, Moraxella* and *Corynebacterium* genera [21,92]. Differently, adult bNM microbiota results more diverse compared to those of infants even though characterized by a smaller bacterial load with high relative abundances of *Corynebacterium spp., Staphylococcus spp., Cutibacterium spp.* genera*,* whereas the bNM in elderly subjects shows a (> 65 years) shifts towards a more oropharyngeal composed bacterial membership [21,92].

The reported variations within the bNM composition are probably linked with the process of aging through the immune senescence mechanism, which is characterized by an increased pro-inflammatory state as well as by a decreased ability to control the activity of the of immune system, together creating suitable environmental niches after partially loss of some residential bacterial strains [93].

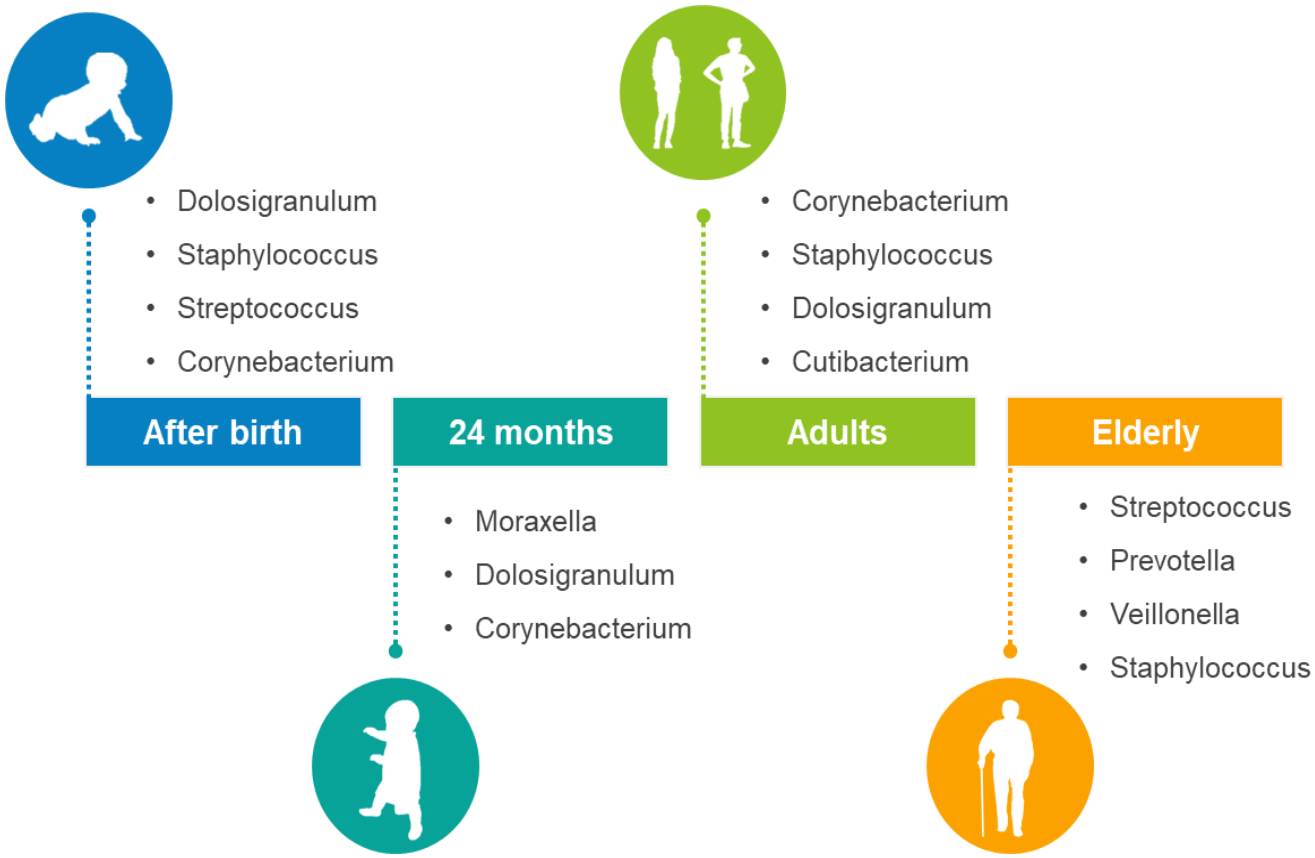

Figure 6. Bacterial nasal microbiota composition during infancy and different age groups. Bacterial genera given in the figure were found at or between the stated time points of life by molecular methods (16S rRNA sequencing with NGS). For references, see [21].

Moreover, the bacteria belonging to other UTR niches are often observed and identified within the bacterial nasal community such as *Moraxella spp. and Streptococcus spp.* [19,94]. In addition, it has been observed that a normal microbial community could interact with human host providing and carrying out different functions which together concur to maintain health conditions [21]. Similar to the other UTR tract bacterial communities, the primary function provided to the host by the bNM consists in heightening the resistance against pathogens colonization [19,92]. Colonization resistance is achieved through competitive exclusion activity of the residential community, directly preventing pathogen adhesion and colonization due to the presence of the indigenous flora, and indirectly competing for

metabolites as well as creating a no-suitable environment for pathogens through catabolism production [95].

In particular in the UTR, the ability of the *Corynebacterium spp.* and *Dolosigranulum spp* to control the rate of proliferation of common respiratory pathobionts such as *S. pneumoniae, H. influenzae, and S. aureus,* especially in younger individuals was documented [96]. Moreover, it has been hypothesized that the respiratory microbiota could train the immune system in early life and assist the local immune homeostasis during the other stages of life, through a fine host-microbiota cross-talk, which has to maintain a delicate balance between the concentration of commensal and pathobiont bacteria inhabiting the respiratory mucosa merged to the constant exposure to environmental stimuli [19].

However, when functional or compositional alterations occur within the bacterial membership, often linked with the effects of different perturbing factors as antibiotic, drug treatment, smoking- and bad habits, and chronic diseases, the functions provided to the host can be altered or ceased leading to an state called dysbiosis, which is often related to different pathological conditions [19,21]. Dysbiosis in the residential bacterial community has been linked to UTR infections, chronic-rhinosinusitis, allergies, asthma, and cystic fibrosis, generally characterized by the loss of beneficial and commensal bacteria which in turns lead to the overgrowth of pathobionts [21,97,98].

THE HUMAN MICROBIOTA ANALYSIS: History and relevant aspects of sequencing based microbiota studies

The first evidence that microbes inhabit the human body was discovered in the midlle-1880s by Theodor Escherich, a pediatrician which identified a bacterium in the intestines of healthy and children affected by diarrhea, named *Escherichia coli*.

Later, studies focused on the human microbiota discovered several other microbes specifically isolated from the skin, oral, nasal and urogenital tract. Even if the positive effects of the residential bacterial community on human health had been firstly observed in the early 1900s, it was only in the end of 20th century when the researcher community gradually realized the healthy role of the microbiota, in particular referring to intestinal microflora, pointing out a possible contribution on the prevention of host infections and cancer [99]. More recently, in 2007 along with the development of the second generation sequencing platforms, it was started a project, called the Human Microbiome Project, that aimed to characterize the composition and the role of the gut bacterial community in a population of 300 healthy volunteers [100]. Up to date, the interest and the number of studies focused on the role of the microbiota in health and disease has been exponentially raised, and the knowledge of microbiota is expanding rapidly.

Sequencing-based analysis continues to be the most common approach among microbiota studies, which is largely afforded by two techniques, both nowadays scaled up to include thousands of samples in a single study: metagenomics or amplicon sequencing [101].

The former technique generally affords a more comprehensive, but also more expensive, taxonomic and functional analyses of the entire microbial community inhabiting a specific district, applying a whole-genome shotgun approach to fragment and sequence the entire genomic material of a microbiome sample.

The latter instead, is based on the selective binding of pangenomic primers to specific conserved regions within the bacterial genomes and the sequencing of the PCR amplicons, generating compositional microbiota data at a more affordable costs. Among the possible marker genes, the most commonly amplified is the bacterial 16s rRNA gene, approximately 1600 base pairs (bp) long and contains nine hypervariable regions (V1-V9), characterized by a variable conservation among bacteria species, that can be used to infer the taxonomic relationships of their microbial hosts, as showed in Figure 7 [102].

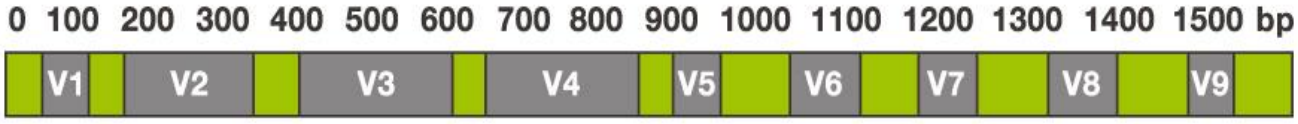

Figure 7. 16S rRNA gene structure exemplification. In the picture conserved and hypervariable regions are colored in green and grey respectively.

After applying different quality filter based approaches, 16S sequences have been usually clustered into operational taxonomic units (OTUs) based on arbitrarily defined thresholds of 97% of sequence similarity so assigning slightly different sequences to the same cluster or bacterial taxon, due to a shared biological origin. Therefore, through this method the effects of technical errors are lowered at cost of decrease sensitivity in identify biological variations, even within the same OTU [103].

To overcome this issue, reference-free statistical denoising methods such as *Deblur or Dada2* have been proposed, generating sequence dataset error profiles, applied to correct technical errors and achieve single-nucleotide resolution, providing, through the analysis of the obtained amplicon sequence variants (ASVs), an higher sensitivity and specificity diminishing the problem of miss-clustered sequences [104,105]. In addition, as ASVs are generated by independent biological sequences and not depend on the dataset from which

they are produced as for OTUs, they allow the reproducibility and comparability of different amplicon-based microbiota studies [106].

Following OTUs or ASVs generation, taxonomic reference-based and both alpha- and beta-diversity analyses are generally performed to inspect the composition of the observed bacterial community and to investigate its ecological characteristics such as microbiota richness, evenness and phylogenetic diversity through appropriate distance indices and metrics, respectively [107].

16S sequence-based studies can be integrated with cultivation-based or different bio-molecular methods such as qPCR, flow-cytometry or the analysis of specific biomarker to further biologically complement the functional and compositional information obtained with the analysis of the sequencer output as well as to investigate possible links with the host homoeostasis [101,108].

However, the increased interest in this field has generated a wide variety of costume protocols, composed by bioinformatics and/or bio-molecular workflows, to analyze the different aspects of the microbiota community, which in most of the cases are not made fully, freely and easily accessible. Therefore, to constantly foster the interest and reliability of the scientific community on the microbiota research, accurate and comprehensive analysis protocols should be provided to allow for full study reproduction, from sample collection to data analysis [101].

PROJECT AIMS

The main aim of the present project is to identify how PM exposure, here chosen as paradigmatic environmental stressor, might modify the homeostasis and composition of the nasal bacterial community and the EV signaling network leading to an alteration of the maternal health and eventually influencing newborn development.

The study population includes 518 healthy pregnant women attending the Fetal Medicine Unit (FMU) of the “Clinica Mangiagalli”- Fondazione IRCCS Ca’Granda – Ospedale Maggiore Policlinico, for routine pregnancy screening during the first trimester. For each study participant, maternal parameters, fetal measures (echography and biochemical measures), birth outcomes and a blood sample to measure EVs (number, size and cellular origin) were collected.

In a subgroup of 65 pregnant women, we investigated additional parameters such as the composition of bacterial nasal microbiota, PM exposure measured by a personal sampler and maternal cardiovascular outcomes.

The specific aims of the present study are described in Figure 8 and include:

AIM 1: To verify the possible effect of PM exposure on fetal and maternal parameters retrieved during routine pregnancy screening in the whole study population (i.e. *fetal parameters*: nuchal translucency thickness, both mean ductus venous and uterine artery pulsatility index; *maternal parameters*: pregnancy-associated plasma protein A (PAPPA and median human chorionic gonadotropin (hCG) concentrations).

AIM 2: To investigate the possible effects of PM exposure on birth outcomes such as the weight and gestational age at birth.

AIM 3: To assess if exposure to PM can alter EVs in plasma as quantity, size and cellular origin in the whole study population (n=518)

AIM 4: To confirm the finding of aim 3 in the subgroup of pregnant women (n=65) in which the measures of air-pollutant concentrations from personal sampler (PS) were available.

AIM 5: To evaluate the associations between personal PM exposure and cardiovascular maternal outcomes, in particular heart rate, diastolic and systolic pressure at rest, in the subgroup of pregnant women (n=65).

AIM 6: To verify if PM levels derived from FARM models and PS devices were associated to bacterial nasal community observed in the subgroup of 65 pregnant women.

AIM 7: To assess the possible role of microbiota pattern (i.e. relative abundance of gram-negative bacteria) in modifying the effect of PM exposure on EVs (see aim 3).

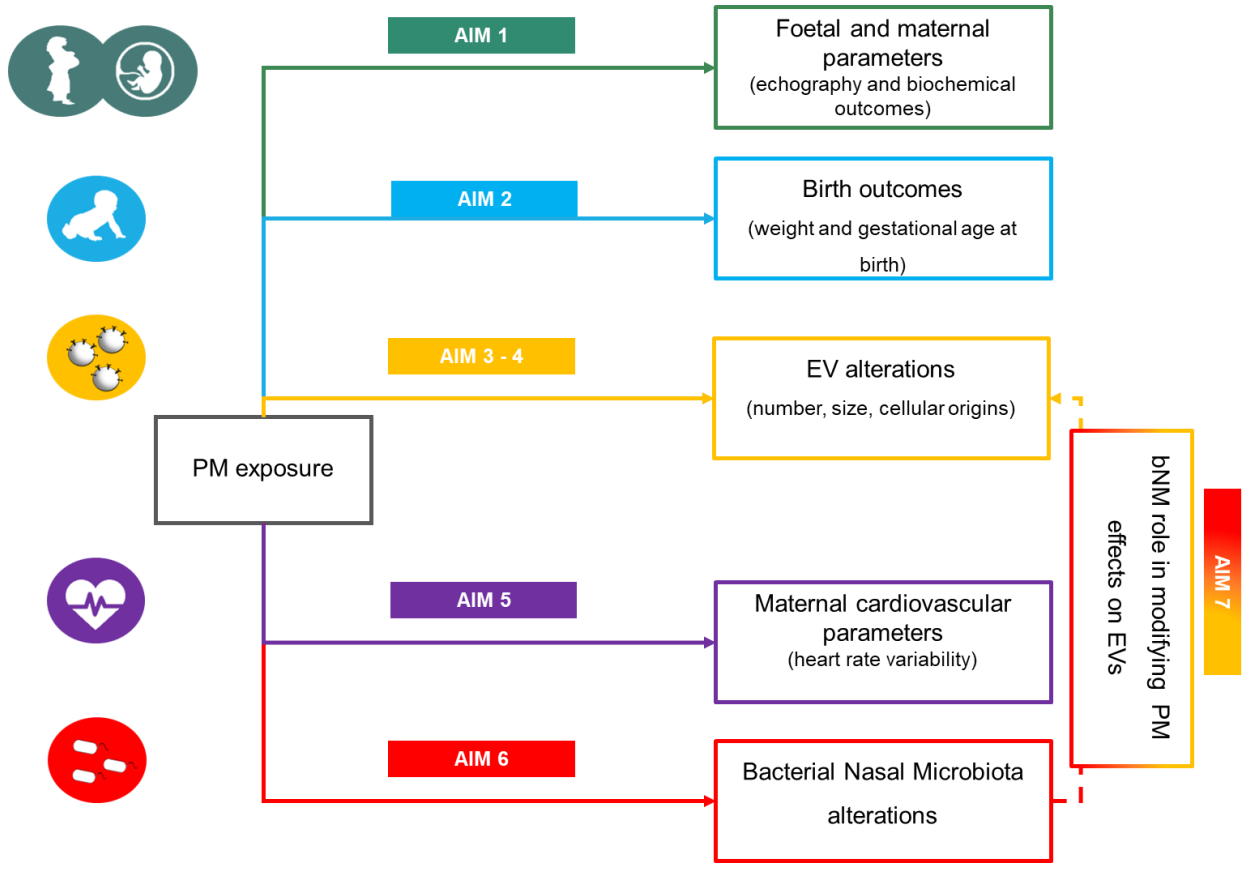

Figure 8. Graphical summary of specific aims for both the whole population (n=518) and the selected subgroup of pregnant women (n=65)

MATERIALS AND METHODS

Subject recruitment and sampling schedule

518 pregnant women were recruited during between July 2014 and July 2019 at the 'Clinica Mangiagalli'-Fondazione IRCCS Ca' Granda – Ospedale Maggiore Policlinico, Milan, Italy.

Each study subject was enrolled approximately during the 11th week of pregnancy. Exclusion criteria included: women with a previously history of illicit drug use, diabetes, hypertension, autoimmune diseases, tumors, recurrent miscarriages, in vitro fertilization, and cardiovascular diseases. Each participant was asked to fill in a standardized questionnaire collecting information about demographics and lifestyle including smoking habits, and alcohol consumption as well as an obstetric history (number of previous pregnancies, twin pregnancy, previous pregnancy complications, and current pregnancy complications).
From each recruited volunteers, a blood sample was collected. Biochemical maternal parameters (pregnancy-associated plasma protein A (PAPPA), human chorionic gonadotropin (hCG) levels), fetal parameters obtained from echography screening, such as nuchal translucency thickness, uterine artery and ductus venous pulsatility indices, were retrieved. Moreover, newborns medical records were collected after delivery from CEDAP (Certificate of delivery care) retrieving data about birth outcomes, such as birth weight and gestational age at birth.

Within the study population, a group of subjects composed by 65 pregnant women, who agreed to participate to a more complex study protocol, was also identified. The same exclusion criteria were applied during the enrolment of this subgroup of pregnant women and an additional evaluation of known cardiovascular risk factors (previous cardiovascular events, hypertension, anemia, and renal failure) was collected, when questionnaires were filled in.

This subgroup of pregnant women was asked to donate a nasal swab right at enrolment (T0), and to return the following Monday (T1) as well as at the 24th week of pregnancy (T2) in order to collect bio specimens (nasal swab and blood) at different time points as well as to attend two cardiovascular screening (T1 and T2) (see Figure 9):

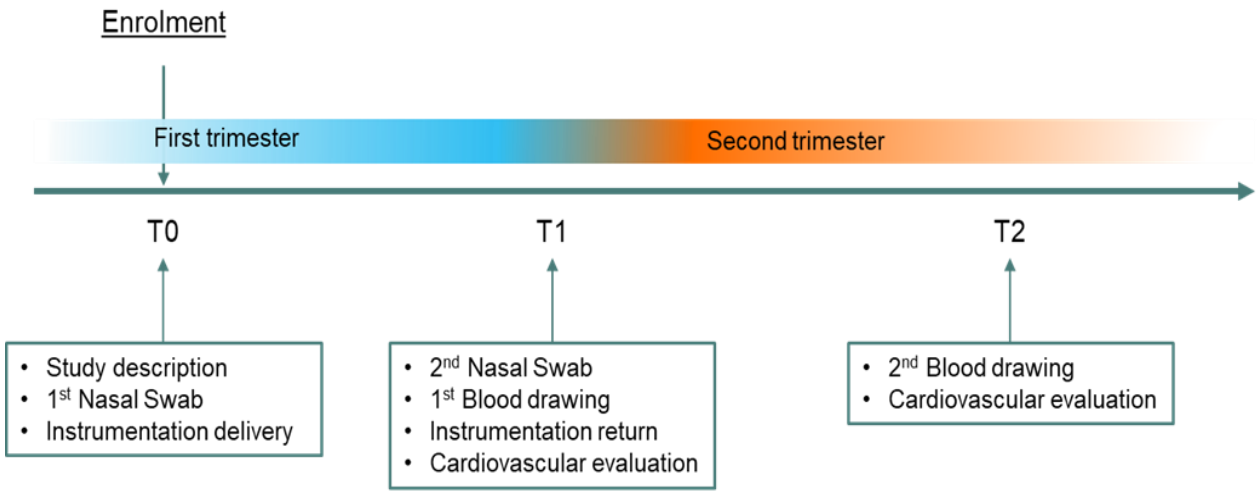

Figure 9. Project sampling timeline for the subgroup of pregnant women (n=65)

The sampling schedule is detailed below:

Time point 0 (T0):

- A first nasal swab specimen for microbiota analysis was collected.
- A personal sampler, to measure individual PM concentration, integrated with a relative humidity device, was delivered to each of the 65 volunteer for exposure data collection.

Time point 1 (T1):

- Collection of the 2nd nasal swab for microbiota analysis
- First blood sample collection for EVs analysis

Time point 2 (T2):

- Second blood sample collection for EVs analysis
- Fetal ultrasound

Each blood drawing consisted in the collection of two EDTA tube containing 7.5ml of blood for each subject.

Collected nasal swabs were immediately placed in a sterile vial and conserved at -80°C for further analysis.

Moreover, at both T1 and T2 time points each of the 65 subject underwent to a cardiovascular evaluation carried out by the 'Dyspnea Lab' unit at Padiglione Sacco – IRCCS Ca' Granda – Ospedale Maggiore Policlinico, Milan, Italy, which included:

I. Blood pressure measurement, at rest, at exercise peak and after exercise loop performed on a semi-recumbent cycle ergometer.
II. Holter-electrocardiography (ECG) to noninvasively evaluate the cardiopulmonary hemodynamic, during and after the exercise stage
III. Doppler echocardiography to assess in a noninvasively way the hemodynamic adaption during the exercise

Particulate matter exposure data collection

Daily air pollutants (PM_{10} and $PM_{2.5}$) concentrations were retrieved from the archives of the Regional Environmental Protection Agency (ARPA Lombardy). Daily PM_{10} and $PM_{2.5}$ concentration were estimated from FARM (Flexible Air quality Regional Model) chemical-physical model of air quality [109]. FARM consists in a three-dimensional Eulerian model that simulates the dispersion and chemical reactions of atmospheric pollutants. The system for the forecast of pollutant concentrations is composed of a meteorological model powered by simulation data. The domain of the simulation with the air quality model FARM covers the Lombard territory in its entirety, with a grid of 1x1Km^2 cells, provided from the website with daily estimates at municipality resolution. Finally, concentration data measured from the stations of the ARPA air quality network is integrated into the simulation results employing interpolation techniques. PM levels estimated at Milan were considered as representative of mean concentrations during the day of enrollment. For all other days, residence exposure was used.

The estimated levels of daily PM_{10} and $PM_{2.5}$, concentrations were assigned to each subject for the day of enrolment, the day before the enrolment, back to the 13 weeks before the blood-drawing, and forward to the delivery date. Subsequently the average exposure from the first week before the visit, for the three trimesters of pregnancy and for the entire pregnancy period were calculated.

The reliability exposure sources have been already assessed and a correlation has been found between FARM and personal sampler (PS) [65], which is considered the gold-standard for PM exposure collection data.

To the group composed by 65 enrolled pregnant women were asked to carry a PS, in order to retrieve personal PM fraction measurements via a portable direct reading monitor

(Aerocet 831-MetOne Instrument Inc., Grant Pass, Oregon, USA- named Personal Sampler (PS)) along with a set of portable instruments for the collection of environmental air pollutant concentration in the breathing zone while moving to the 'Dyspnea Lab' unit at Padiglione Sacco – IRCCS Ca' Granda – Ospedale Maggiore Policlinico, Milan, Italy, to attend the cardiovascular evaluation at T1.

The delivered devices were asked to be worn starting from Monday morning until the cardiovascular vascular evaluation at T1.

To improve data quality, comparative sessions between a freshly calibrated PS and a gravimetric cold standard for PM fractions (Harvard Impactor MS&T Area Sampler Diagnostic and Engineering, Harrison, ME, USA) were performed.

Plasmatic EV analysis: Isolation & purification

For the isolation and purification of the plasmatic EV fractions the following validated protocol was applied to each collected blood sample.

Two 7.5 ml blood drawing specimens were collected into EDTA tubes for each subject at and processed within 2 hours from the phlebotomy in order to avoid EV degradation.

Each blood sample underwent serial centrifugations in order to be cleaned up, followed by an ultracentrifugation step to obtain a free EVs-rich pellet for the following EV analyses.

Centrifugation steps to obtain the EV-rich pellet were accomplished as follow:

I. Serial plasma centrifugations at 1000, 2000 and 3000*xg* for 15 min at 4°C to remove cell debris. The pellet was discarded to remove cell debris.
II. A volume of 1.5 ml of fresh plasma was transferred to 13.5 ml ultracentrifuge tube (Beckman Coulture), which was filled up with PBS filtered through a 0.1 µm pore size (StericupRVP, Merk Millipore) in order to minimize background particle contribution.

The tube successively underwent to ultracentrifugation step (Beckman Coulter Optima-MAX-XP) at 110,000*xg* for 75 minutes at 4°C to obtain EVs-rich pellet.

Each retrieved EV-rich pellet was then suspended in 550 µl of triple-0.1 µm pore size-filtered PBS to undergo immunophenotypization assay and nanoparticle tracking analysis, via flow cytometer and Nanosight NS300 system respectively.

Plasmatic EVs analysis: EV immunophenotypization and flow-cytometry analysis

Immunophenotypization assay was performed to each EV-rich pellet in order to identify the EV cellular origin using a flow cytometer (MACSQuant, Miltenyi Biotec) according to a standardized protocol [110]. Before the EV analysis, to proper set the instrumentation, a step of gating calibration was carried out using Fluoresbrite® Carboxylate Size Range Kit I (0.2, 0.5, 0.75, and 1 µm).

The first step of immunophenotypization analysis consisted to assess EV integrity through carboxyfluorescein diacetate N-succinimidyl ester (CFSE) staining. CFSE is a cell permeant, non-fluorescent pro-dye, which produces fluorescent reaction when intracellular esterases remove the acetate groups and convert the molecule to the fluorescent ester. CFSE labelled EVs can be detected through the flow cytometer FITC detection channel. 60 µl of each sample aliquot was stained with 0.02 µM CFSE at 37 °C for 20 min in the dark.

The second step was characterized by specific antibody staining to assess EV-cellular origin. For each subject, seven 60 µl CFSE stained aliquots were processed using a specifically-chosen antibody at time.

The following panel of antibodies (Miltenyi Biotec) was used:

Antibody	Clone	EV origin
CD-14-APC	clone TÜK4	Macrophages/Monocytes
CD105-APC	clone 43A4E1	Endothelial cells
CD62E-APC	clone REA280	Activated endothelial cells
CD61-APC	clone Y2/51	Platelets
CD25-APC	clone PC61	Regulatory T cells
HLA-g-APC	clone MEM-G/9	Trophoblast
Herv-W-APC	clone 4F10	Syncytin-1 protein

The antibodies used to characterized EVs were chosen due to the relevance of the respective cell-type in inflammatory reaction (CD61+, CD105+, C25+, CD62E+, CD14+), which are set up by PM exposure, as well as to their role in placentation (HLA-g+ and HERV-w+).

After adding the single antibody, each aliquot was incubated for 20 minutes at 4°C in the dark. Each chosen antibody was previously centrifuged at 17.000xg at 4°C to eliminate aggregates before adding it to the sample and autofluorescence of the antibodies was assessed using a PBS stained control.

Quantitative multiparameter analysis of flow cytometry data was carried out by using FlowJo Software (Tree Star, Inc.).

Plasmatic EV analysis: Nanoparticle tracking Analysis

Nanoparticle tracking analysis (NTA) is a technique applied to visualize and analyze nanoparticles in suspension, ranging from 10-1000 nm based on that measurement of the Brownian motion. NTA allows the direct measurement of the concentration as single particles in the illuminated volume such as vesicles suspended in fluid, and displays them in real time through a CCD camera with high sensitivity, calculating the size of each individually tracked particle, thus simultaneously allowing determination of nanoparticle size distribution and concentration.

In this study NTA was applied to retrieve the numbers and dimensions of EVs through the Nanosight NS300 system (NanoSight Ltd., Amesbuty, UK). In order to perform NTA, 100µl of the EV-rich resuspended pellet was diluted with triple-0.1 µm pore size-filtered PBS to at least 300µl, which is the minimum volume to perform NTA analysis using the NS300 low volume chamber.

Each sample underwent to a five 30s recording using the light scattering mode.

The NS300 output consists in a .csv file containing the EV concentration for each size, ranging from 0.5 nm to 999.5 nm. Due to EV biological features, only the data spanning from 30nm to 700nm were took into account for further analyses.

Microbiota analysis: nasal swab collection and sample processing

Nasal swabs were collected both at T0 and T1 from each of the 65 selected subjects following WHO guidelines (https://goo.gl/pMzSrT), for a total of 130 swabs. In detail, a dry polyester swab is inserted into the nostril, close to the nares external mucosa, and left in place for a five seconds and then slowly withdrawn with a rotating motion. Specimens from both nostrils are obtained with the same swab. The tip of the swab is put into a plastic vial and stored at -80°. DNA was then extracted using QIAamp® UCP Pathogen Mini (QIAGen, Hilden, Germany) following manufacturers guidelines. The obtained DNA was stored at -20°C and later the samples were shipped to the sequencing service facility Personal Genomics Srl (Verona, Italy) to perform qualitative and quantitative checks, PCR amplification and second-generation sequencing analysis, including libraries preparation. The bacterial nasal membership was investigated through the metabarcode sequencing analysis of the 16S rRNA gene regions V3-V4, amplified with the primer pair Pro341F (5′-CCTACGGGNBGCASCAG-3′) and Pro805R (5′-GACTACNVGGGTATCTAATCC-3′), and then sequenced through the Illumina MiSeq platform using a paired-end library of 300bp insert size.

Microbiota analysis: sequencer output upstream analysis

The obtained demultiplexed sequencer outputs were checked for reads quality control and statistics using the software FastQC v0.11.2. Then through a *.tsv* file, containing the sample ID and absolute path information of each reads archives, the DNA sequence data containing both the forward and the reverse reads of each subjects were imported into the QIIME 2 v2020.6 software for the following analysis [107]. Primer sequences were removed from each read with the *cutadapt* plugin using the *trim-paired method* to avoid possible following database mismatches due to the presence of the primer sequences within each reads. Each

file containing the forward reads were then joined to the corresponding reverse reads file using *Vsearch's merge_pairs* function with a minimum overlap length of forward and reverse reads of 80 bp for joining [111], to cover the total length of the 16S V3-V4 hypervariable regions. Successively, a quality filtering process was applied on the joined-reads filtering all the sequences with a quality value less than a PHRED score of 20 on a base-slide window of 3 nucleotides. The retained sequences were then grouped into high-resolution amplicon sequence variants (ASVs) using the *Deblur denoiser plugin* with an arbitrary minimum length of 400bp to be retained [104]. Taxonomic assignment was done with the *skylearn-classifier* against the SILVA v132_99_16S, which had been modified to contain only the V3-V4 16S fragments to improve read matching. *Mafft-fast-tree method* and default settings suggested in QIIME 2 pipeline were applied to align sequences and generate rooted and unrooted trees for phylogenetic analysis. The resulting ASVs or feature table and phylogenetic tree were used for the following analysis.

Microbiota analysis: downstream analysis

Downstream analyses were also carried out using QIIME2 v2020.6 on the obtained feature table. Additional filtering steps were performed, removing features found in less than 15 sample as well as removing all the subjects with a total sequence number less than 2000 reads according to rarefaction curves analysis. Moreover, feature table was normalized by 16S copy number (GCN) based on *rrn*DB database (version 5.6). Taxonomic values was assigned to each ASV from the phylum to the genus level. To assess significant differences among the identified ASVs in the analyzed groups, DSFDR and ANCOM software were applied. DSFDR achieve high statistical power to detect significant findings in sparse and noisy microbiota data compared to the commonly used Benjamini-Hochberg procedure and other FDR-controlling procedures. On the other hand, ANCOM software, which stand for analysis of composition of microbiomes, accounts for the underlying structure in the data

and can be used for comparing the composition of microbiota in two or more populations. Alpha-diversity values were calculated using observed ASVs, Shannon and Faith's phylogenetic_diversity (Faith's PD), in order to retrieve information about the within diversity of each sample at T0 and T1, and a Kruskal-Wallis test was applied to assess possible differences between time points. Beta-diversity was examined applying the Weighted_Normalized UniFrac distance measure. In addition, Principal Coordinate Analysis (PCoA) were generated on the produced distance matrix and plotted using Emperor and PERMANOVA test with 999 permutations function was applied to test significance in dissimilarity matrices between T0 and T1 groups, comparing the tightness of clusters within all samples in a group.

Graphical visualization of the data were performed using Seaborn v0.11.0, a Python data visualization library based on matplotlib, which provides a high-level interface for drawing attractive and informative statistical graphics.

To perform these analysis and the ones reported in the paragraph above the following commands were run in a Conda environment (https://docs.conda.io/en/latest/) containing the whole dependencies and programs needed for QIIME2 workflows, using the Ubuntu 18.04 LTS terminal for Windows 10 and applied in this order:

- *qiime tools import --type 'SampleData[PairedEndSequencesWithQuality]'* &
- *qiime demux summarize &*
- *qiime cutadapt trim-paired &*
- *qiime vsearch join-pairs &*
- *qiime quality-filter q-score-joined &*
- *qiime metadata tabulate &*
- *qiime deblur denoise-16S &*
- *qiime feature-table summarize &*

- *qiime phylogeny align-to-tree-mafft-fasttree&*
- *qiime feature-classifier classify-sklearn &*
- *qiime taxa collapse &*
- *qiime feature-table relative-frequency &*
- *qiime gcn-norm copy-num-normalize &*
- *qiime diversity alpha-rarefaction &*
- *qiime diversity alpha*
- *qiime diversity beta &*
- *qiime emperor plot &*
- *qiime diversity alpha-group significance &*
- *qiime diversity beta-group significance &*
- *qiime dsfdr permutation-fdr &*
- *qiime composition add-pseudocount &*
- *qiime composition ancom &*

Comprehensive descriptions of each command can be found at https://docs.qiime2.org/2020.8/plugins/ and each underlying python code are freely accessible at https://github.com/qiime2/ repository.

Statistical Analysis

Descriptive statistics were performed on all variables. Continuous variables were expressed as the mean ± standard deviation (SD) or as the median with first-, and third-quartile (Q1–Q3), as appropriate. Categorical data were reported as frequencies with percentages. The comparison of patients' characteristics between the total population (n=518) and the subset of the woman with a personal sampler (n=65) was performed with Pearson’s chi-square test for continuous variables and Chi-square test or Mann-Whitney U-test for categorical variables, as appropriate.

To evaluate PM exposure on maternal and fetal parameters derived from echography and biochemical analysis, multivariable linear regression models adjusted for age, BMI, smoking habits, temperature, season, humidity, and gestational age at enrolment, were applied on the whole study population.

To evaluate the association between PM exposure and newborns outcomes multivariable linear regression models adjusted for age, BMI, season, temperature and humidity of the same period of exposure were used. The model to evaluate the association with birth weight was also adjusted for terms vs preterm pregnancy.

In addition, the association of both PM (from FARM and PS) exposure on EV data was evaluated. Because outcomes EV variables are expressed as a concentration, negative binomial regression models for count data with over-dispersion to model EVs and cell origins as a dependent variable were done. The models were adjusted for age, BMI, smoking habits, temperature, humidity, and gestational age at enrolment. The presence of over-dispersion was tested by the likelihood ratio test.

To evaluate the relationship between pollutant exposure (from both the FARM model and PS) and cardiovascular outcomes on the subgroup of 65 pregnant women, we applied multivariable regression models adjusted for age, BMI, and gestational age at enrolment.

The association between PM (from FARM and PS) exposure on bNM was also evaluated, in terms of alpha-diversity, proportion of gram- negative bacteria, and relative abundance (RA) of the most represented bacterial genera. The models were adjusted for age, BMI, and gestational age at enrolment. Women were stratified according to their %RA of gram-negative (categorized as Gram- ≤ 20% and Gram- > 20%). The mean differences between the two groups of %RA of gram-negative in terms of the distribution of vesicle mean concentrations for each EV size were analyzed. Firstly, the EV mean concentration at each size, with multivariable negative binomial regression models, independently from PM exposure was estimated. Secondly, the adjusted EV marginal mean between the two groups of subjects was compared. False Discovery Rates (FDR) values were calculated using the multiple comparison methods based on Benjamini-Hochberg FDR that takes into account the high number of comparisons. Results were reported as a series graph for EV mean concentrations of each size and vertical bar charts to represent the p-values obtained comparing Gram- ≤ 20% and Gram- > 20% groups.

We investigate the potential role of bNM as an effect modifier of the association between PM concentration and EVs. The model was adjusted for age, BMI, season, gestational age at sampling, temperature, humidity, and the interaction between PM exposure and categorical gram-negative variable. To produce the estimate and the plot, selected values for exposure and other covariates (mean value or reference categories) have been chosen. These have been incorporated into the equation along with the range of values for PM.

The linearity of the model with interaction has been tested as a step for defining the best model. Each model was tested for normality and linearity. Best model selection was based

on the minimization of the Akaike information criterion and maximization of the explained variance of the model.

Estimated effects are reported as percent variation ($\Delta\% = (\exp(\beta*10) - 1) * 100$) or $\beta*10$ and 95% confidence interval error (CI) associated with an increase of 10 units in each pollutant.

For each applied model, either a p-value <0.05 or a q-FDR ≤ 0.15 were considered as statistically significant (two-tailed).

Statistical analyses were performed with SAS software, version 9.4.

RESULTS

Characteristics of the enrolled subjects

The main characteristics of the overall study population and the selected subgroup are listed in Table 2. In the whole population, the mean maternal age at recruitment, was 33.8 years (± 4.3 years) and the mean gestational was 11.9 weeks (± 0.7 week). Subject enrolment was conducted all over the year: 31.1%, 22.4%, 19.3 %, and 27.2% of the pregnant participants were recruited during the winter, spring, summer, and autumn seasons, respectively. The mean maternal BMI was 22.4 ± 3.7 Kg/m^2; 9.8% of the women were underweight (BMI < 18.5), 69.8% were lean (18.5 ≤ BMI < 25), and 4.8% overweight (BMI ≥ 25). Most women were never smokers (84%), 10.6% quitted smoking at the beginning of gestation and 4.8% declared to be current smoker. The percentage of women at their first pregnancy (60.8%) was higher than the one of woman who has given birth two or more times (38.8%). Moreover, the levels of the tested gestational associated endocrine factors showed a median plasma protein A (PAPPA) of 2.8 IU/l (Q1, Q3: 1.8-4.0) and a median human chorionic gonadotropin (hCG) concentration of 46.3 IU/l (Q1, Q3: 30.2-70.2). Fetal parameters were also collected during echography screenings, such as crown-rump length, nuchal translucency thickness, fetal heart rate, ductus venous pulsatility index (DVPIV), blood pressure, and uterine artery pulsatility index (UtaPI) and their mean values are reported in Table 2. Newborn mean gestational age at birth was 39.3 weeks (± 2.2 weeks) and average weight at birth was 3248.9 gr (± 451 gr).

The subgroup of 65 pregnant women presented similar characteristics of the whole population with possible exceptions for mean gestational age at recruitment (slightly higher), enrolment seasonality, gestational age and weight at birth, mean crown-rump length and the average DVPI.

Table 2 Characteristics of the study participants (N = 518) and the subgroup of women with personal sampler (N= 65).

Characteristic	Total population (n=518)	Subgroup of woman with personal sampler (n=65)	*P-value*
Age, mean ± SD, year	33.8 ± 4.3	33.9 ± 3.5	0.876
Gestational age at sampling, weeks	11.9 ± 0.7	12.4 ± 1.0	<0.001
Cardiovascular features			
Rest diastolic pressure	-	62.0 ± 8.9	
Rest systolic pressure	-	97.3 ± 11.1	
Rest heart rate	-	30.9 ± 9.5	
Season of enrolment, n (%)			
winter	161 (31.1%)	38 (58.5%)	
spring	116 (22.4%)	15 (23.1%)	<0.001
summer	100 (19.3%)	0 (0%)	
autumn	141 (27.2%)	12 (18.5%)	
Anthropometric and biochemical features			
BMI, Kg/m²	22.4 ± 3.7	22.5 ± 3.4	0.842
Categorical BMI			
Underweight (BMI < 18.5)	50 (9.8%)	5 (7.7%)	
Lean (18.5 ≤ BMI < 25)	358 (69.8%)	49 (75.4%)	0.657
Overweight (BMI ≥ 25)	105 (20.5%)	11 (16.9%)	
Smoking habits, n (%)			
Never smoked	435 (84.0%)	61 (93.9%)	
Stopped during pregnancy	55 (10.6%)	2 (3.1%)	0.123
Smoker	25 (4.8%)	2 (3.1%)	
Features related to pregnancy			
Parity			
Nulliparity	315 (60.8%)	40 (61.5%)	0.958
Multiparity	201 (38.8%)	25 (38.5%)	
Pregnancy associated endocrine factors			
PAPPA, IU/L, median (Q1, Q3)	2.8 (1.8-4.0)	3.0 (1.7-4.6)	0.689
hCG, IU/L	46.3 (30.2-70.2)	50.5 (33.5-67.5)	0.715
Fetal parameters			
Crown-rump length	62.8 ± 6.4	65.3 ± 59.3	0.002
Nuchal translucency thickness	1.9 (1.6-2.1)	1.9 (1.7-2.2)	0.132

Fetal heart rate	160.3 ± 7.3	161.2 ± 13	0.608
Ductus venous pulsatility index	1.0 ± 0.2	1.0 ± 0.1	0.043
Mean blood pressure, mmHg	85.8 ± 7.5	85.6 ± 7.8	0.809
Mean UtaPI, mmHg	1.6 ± 0.4	1.6 ± 0.4	0.861
Neonatal parameters			
Weight at birth (g)	3248.9 ± 451	3389 ± 365.3	0.037
Gestational age at birth (week)	39.3 ± 2.2	39.7 ± 1.1	0.043

For normal distributions, continuous values are expressed as mean ± standard deviation, conversely values are expressed as medians (Q1, Q3). Categorical values are listed as frequencies with percentages. Data are missing for some variables. BMI=body mass index; hCG=human chorionic gonadotropin; PAPPA=pregnancy-associated plasma protein-A.

Descriptive statistics of particulate pollutant concentrations, deriving from both FARM models and personal sampler (PS) for each considered exposure lag-windows are reported in Table 3.

Table 3 Summary of the descriptive statistics of the air-born particles concentration data measured by FARM models and personal sampler (PS) for each considered exposure-window

Data provenance	Exposure	Mean	SD	Median	Q1-Q3
FARM models	**PM10**				
	Day 0	42.2	22.9	38.4	25.7-52.7
	Day -1	37.9	21.1	33	22.2-47.7
	1 wk	35.5	14.7	33	24-46
	13 wks	35.4	11.3	35	25-45
	PM2.5				
	Day 0	30.3	15.6	29.3	17.6-38.5
	Day -1	29.2	13.5	27.8	18.4-36.9
	1 wk	26.3	10.5	25	17-35
	13 wks	27.9	8.3	29	20-35
Personal Sampler	***Mean of exposure 1h30 before***				
	PM_1	17.5	13.7	14	8.1-25.4
	$PM_{2.5}$	26.3	18.6	19.7	12.7-36.8
	PM_4	35.2	22.6	27.1	18.7-49.7
	PM_{10}	63.2	43.8	48	30.8-86.2
	TSP	81.4	56.2	63.4	42.1-105.3

Particulate matter exposure effects on maternal and fetal parameters in the whole study population (n=518)

To verify the possible effect of PM exposures, multiple regression models were applied on echography and biochemical parameters in the whole population (n=518). Different exposure lag-windows for PM exposure were considered to achieve a more detailed overview of the effects of air pollution, as reported in Table 4.

Associations between levels of exposure and parameters collected during the echography screening were observed. Mean PM_{10} concentrations were positively associated with both meanUtaPI (PM_{10}-13wks, Δ%=5.21, P 0.01) and DVPI indices (PM_{10}-1wk, Δ%=3.57, P 0.01). Positive association were further observed between 1wk $PM_{2.5}$ mean concentrations and meanUtaPI ($PM_{2.5}$-1wk, Δ%= -4.51, P 0.04) and DVPI parameter values ($PM_{2.5}$-1wk, Δ%= 6.36, P 0.04). Interestingly, DVPI index was the only tested dependent variable to be positively associated with means $PM_{2.5}$ levels of both the day of blood-sample collection (Day 0) and the previous one (Day -1), ($PM_{2.5}$-Day 0, Δ%= 4.61, P 0.03; $PM_{2.5}$-Day -1, Δ%= 5.18, P 0.02).

Table 4. Associations between PM concentrations obtained from FARM models and fetal outcomes

Outcome	Exposure	Δ%	LCI	UCI	*P-value*
Echography parameters					
Nuchal translucency	**PM_{10}**				
	Day 0	0.28	-0.87	1.44	0.64
	Day -1	-0.51	-1.75	0.74	0.42
	1 wk	-0.69	-2.29	0.94	0.40
	13 wks	-0.19	-3.05	2.76	0.90
	$PM_{2.5}$				
	Day 0	-0.41	-2.60	1.84	0.72
	Day -1	-1.20	-3.51	1.16	0.32
	1 wk	-1.99	-5.23	1.36	0.24
	13 wks	-1.30	-6.44	4.14	0.63
MeanUtaPI	**PM_{10}**				
	Day 0	0.62	-0.90	2.15	0.43
	Day -1	0.46	-1.17	2.12	0.58
	1 wk	-0.37	-2.47	1.78	0.74
	13 wks	5.21	1.31	9.25	**0.01**
	$PM_{2.5}$				
	Day 0	0.55	-2.34	3.53	0.71
	Day -1	-1.15	-4.13	1.93	0.46
	1 wk	-4.51	-8.58	-0.26	**0.04**
	13 wks	2.89	-3.98	10.26	0.42
DVPI	**PM_{10}**				
	Day 0	1.85	-0.09	3.82	0.06
	Day -1	2.07	-0.04	4.21	0.05
	1 wk	3.57	0.75	6.48	**0.01**
	13 wks	-0.24	-5.18	4.96	0.93
	$PM_{2.5}$				
	Day 0	4.61	0.56	8.82	**0.03**
	Day -1	5.18	0.79	9.77	**0.02**
	1 wk	6.36	0.19	12.92	**0.04**
	13 wks	-1.91	-10.79	7.85	0.69

Results from multivariate regression models on the total population (n=518). Association between both PM concentration and the tested parameters were adjusted for age, BMI, Smoking habits, season, temperature, humidity, gestational age at sampling. Nuchal translucency, DVPI dependent variables are log transformed. Bold P values underline statistical significance. A Δ% = (exp (β) −1) * 100, percent variation of each parameters for 10 μg/m^3 increase for the considered pollutants. LCI and UCI = lower and upper confidence interval.

Beside the echography-derived data, maternal biochemical parameters were also tested for statistical relationships with the same PM lag-windows. Although no associations were found between PM concentrations and hCG serum values, Day 0 PM_{10} levels were positively associated with PAPPA screened amount (Day 0 PM_{10}, Δ%= 4.66, P <0.01;), as showed in Table 5.

Table 5. Associations between PM concentrations obtained from FARM models and maternal outcomes.

Outcome	Exposure	Δ%	LCI	UCI	*P-value*
Biochemical parameter					
	PM_{10}				
	Day 0	4.66	1.51	7.91	**<0.01**
	Day -1	2.40	-0.84	5.75	0.15
	1 wk	5.29	-0.05	10.92	0.05
	13 wks	6.33	-2.97	16.51	0.19
PAPPA	**$PM_{2.5}$**				
	Day 0	5.19	-1.27	12.08	0.12
	Day -1	2.76	-5.49	11.73	0.52
	1 wk	0.78	-10.86	13.93	0.90
	13 wks	3.64	-12.85	23.24	0.69
	PM_{10}				
	Day 0	-1.42	-4.20	1.43	0.32
	Day -1	-0.95	-3.87	2.05	0.53
	1 wk	-2.92	-7.50	1.90	0.23
	13 wks	0.26	-7.91	9.15	0.95
hCG	**$PM_{2.5}$**				
	Day 0	-0.19	-5.32	5.21	0.94
	Day -1	-1.06	-7.69	6.05	0.76
	1 wk	-1.96	-11.44	8.53	0.70
	13 wks	10.93	-3.85	27.99	0.15

Results from multivariate regression models on the total population (n=518). Association between both PM concentration and the tested parameters were adjusted for age, BMI, Smoking habits, season, temperature, humidity, gestational age at sampling. PAPPA levels are log transformed. Bold P values underline statistical significance. A Δ% = (exp (β) −1) * 100, percent variation of each parameters for 10 μg/m^3 increase for the considered pollutants. LCI and UCI = lower and upper confidence interval.

Particulate matter exposure effects on newborns outcomes in the whole study population (n=518)

PM concentration were further tested to assess potential association with both newborn weight and gestational age at birth in the whole study population (n=518), as showed in Table 6.

Although no associations were found between PM exposure and birth weight values, mean PM_{10} concentrations of either the whole gestational period (All pregnancy) or the 2nd trimester showed negative associations with the gestational age at birth (PM_{10}-All pregnancy, Δ%= -2.95, P 0.009; PM_{10}-2nd trimester, Δ%= -24.97, P 0.017), the latter also with effects almost 9-folds. Consistently, the levels measured for the fine PM fraction ($PM_{2.5}$) in the 2nd trimester of gestation were also negatively associated with the above considered parameter ($PM_{2.5}$-2nd trimester, Δ%= -3.97, P <0.001).

Table 6. Associations between PM concentrations obtained from FARM models and newborn outcomes

Outcome	Exposure	Δ%	LCI	UCI	*P-value*
Birth weight	**PM_{10}**				
	All pregnancy	-2.41	-6.29	1.62	0.236
	1st trimester	0.15	-2.24	2.60	0.902
	2nd trimester	-2.98	-6.43	0.60	0.101
	3rd trimester	-1.93	-4.57	0.77	0.159
	$PM_{2.5}$				
	All pregnancy	0.24	-3.17	3.77	0.892
	1st trimester	1.14	-2.45	4.86	0.536
	2nd trimester	-1.84	-6.33	2.86	0.434
	3rd trimester	-2.22	-6.19	1.91	0.286
Gestational age at birth	**PM_{10}**				
	All pregnancy	-2.95	-5.09	-0.75	**0.009**
	1st trimester	-0.26	-1.60	1.09	0.700
	2nd trimester	-24.97	-40.68	-5.11	**0.017**
	3rd trimester	-0.21	-1.54	1.14	0.759
	$PM_{2.5}$				
	All pregnancy	-0.73	-2.11	0.67	0.303
	1st trimester	1.69	-6.70	10.84	0.702
	2nd trimester	-3.97	-5.80	-2.12	**<0.001**
	3rd trimester	-1.44	-3.27	0.42	0.127

Results from multivariate regression models on the total population (n=518). Associations between considered PM fraction concentration and the weight at birth were adjusted for age, BMI, season, temperature, humidity, and term VS preterm pregnancy. Associations between considered PM fraction and the gestational age at birth were adjusted for age, BMI, season, temperature, and humidity. Bold P values underline statistical significance. A Δ% = (exp (β) −1) * 100, percent variation of each evaluated parameters for 10 μg/m^3 increase for the considered pollutants. LCI and UCI = lower and upper confidence interval.

Particulate matter exposure effects on EV concentrations in the whole study population (n=518*)*

Multivariable negative binomial regression models were applied to the EV data obtained from both flow-cytometer (FC) and nanoparticle tracking analysis (NTA) to verify possible relationship with the tested exposure-windows in the whole study population.

Negative associations were observed between each evaluated PM_{10} exposure windows and the total amount of circulating EVs (Sum of EVs) (Table 7), pointing out the strongest effect related to the PM concentration measured 13 weeks before the enrolment (PM_{10}-13wks, $\Delta\%$= -16.21, P <0.001).

Table 7. Associations between PM concentrations obtained from FARM models and NTA data

Outcome	Exposure	Δ%	LCI	UCI	*P-value*
Extracellular vesicles					
Sum of EVs	**PM_{10}**				
	Day 0	-6.74	-9.19	-4.23	**< 0.001**
	Day -1	-4.61	-7.45	-1.68	**0.001**
	1 wk	-12.78	-16.71	-8.65	**< 0.001**
	13 wks	-16.59	-23.25	-9.36	**< 0.001**
	$PM_{2.5}$				
	Day 0	4.74	-0.15	9.86	0.057
	Day -1	5.02	-0.67	11.04	0.15
	1 wk	4.34	-4.08	13.50	0.35
	13 wks	12.79	-0.40	27.74	0.057

Results from multivariable negative binomial regression models on the total population (n=518). Association between both PM concentration and the NTA data were adjusted for age, BMI, Smoking habits, season, temperature, humidity, gestational age at sampling. Bold P values underline statistical significance. A Δ% = (exp (β) −1) * 100, percent variation of each evaluated parameters for 10 μg/m^3 increase for the considered pollutants. LCI and UCI = lower and upper confidence interval.

Flow Cytometry data were tested to get information about the effect of the considered pollutants on possible variations in plasmatic concentration of EVs released from specific cells type, involved in either inflammatory/immunity or gestational processes (Table 8).

The endothelial-derived EV subtypes (CD105+ and CD62E+) showed associations with both PM_{10} and $PM_{2.5}$ levels. CD105+ EVs resulted positively associated with both PM_{10}- Day 0 and the levels measured the week before the blood drawing (1wk) (PM_{10}-Day 0, Δ%= 4.48, P <0.001; PM_{10}-1wk, Δ%= 6.16, P 0.015) whereas PM_{10} concentrations measured the first trimester of gestation (13wks) showed a negative association with CD62E+ EVs (PM_{10}-13wks, Δ%= -19.21, P <0.001). The same exposure-window (13wks) was found to be negatively associated with both those EVs when $PM_{2.5}$ levels were considered ($PM_{2.5}$-13wks: CD105+, Δ%= -22.87, P 0.02; CD62E+ Δ%= -24.68, P <0.001) and a positive association was additionally identified for CD62E+ and $PM_{2.5}$-Day -1 concentrations $PM_{2.5}$-Day-1, Δ%= 7.01, P 0.039).

The concentrations of EVs derived from cells involved in immune processes, macrophages- (CD14+) and regulatory T cells (Treg) (CD25+), showed negative associations with both PM_{10}- and $PM_{2.5}$- 13wks levels (CD14+: PM_{10}-13wks, Δ%= -12.89, P 0.03; $PM_{2.5}$-13wks, Δ%= -33.46, P 0.003; CD25+: PM_{10}-13wks, Δ%= -25.63, P <0.001; $PM_{2.5}$-13wks, Δ%= -33.36, P <0.001). Moreover, a positive association was found between $PM_{2.5}$-Day -1 and the amount of CD25+ circulating vesicles ($PM_{2.5}$-Day-1, Δ%= 7.89, P 0.022).

Consistently with the results found for both endothelial- and immunity-related EVs, PM_{10}- and $PM_{2.5}$- 13wks concentrations were negatively associated with trophoblast-derived EVs (HLA-g+) (PM_{10}-13wks, Δ%= -9.8, P 0.016; $PM_{2.5}$-13wks, Δ%= -29.42, P <0.001). In addition, a negative association was identified for the plasmatic concentrations of this EV subtype and the $PM_{2.5}$- Day 0 levels ($PM_{2.5}$-Day 0, Δ%= -5.66, P 0.025).

It should be noted that syncytin-1 protein positive EVs (HERV-w+) was the only analyzed vesicle subtype sharing positive associations with each PM_{10} tested exposure ($P \leq 0.001$), expressing also a negative association with $PM_{2.5}$-13wks concentrations ($PM_{2.5}$-13wks: $\Delta\% = -31.06$, $P < 0.001$), as for any tested EV subtype except for those derived from platelets (CD61+).

Table 8. Associations between PM concentrations obtained from FARM models and flow-cytometry data.

Outcome	Exposure	% change	LCI	UCI	*P-value*
EV type					
	PM_{10}				
	Day 0	-0.83	-4.24	2.70	0.643
	Day -1	-1.11	-4.68	2.60	0.554
	1 wk	-3.27	-8.94	2.76	0.283
CD61+ (Platelets)	13 wks	-6.80	-16.44	3.95	0.205
	$PM_{2.5}$				
	Day 0	0.71	-6.79	8.82	0.857
	Day -1	6.00	-3.16	16.04	0.205
	1 wk	6.68	-6.77	22.07	0.347
	13 wks	-10.73	-28.05	10.75	0.301
	PM_{10}				
	Day 0	4.88	1.94	7.90	**0.001**
	Day -1	2.93	-0.03	5.98	0.051
	1 wk	6.16	1.15	11.43	**0.015**
CD105+ (Endothelium)	13 wks	5.49	-3.38	15.17	0.233
	$PM_{2.5}$				
	Day 0	1.89	-3.83	7.95	0.525
	Day -1	1.91	-4.81	9.10	0.587
	1 wk	-3.16	-12.53	7.21	0.536
	13 wks	-22.87	-34.01	-9.84	**0.001**
	PM_{10}				
	Day 0	-0.74	-4.83	3.53	0.730
	Day -1	3.51	-1.62	8.91	0.184
	1 wk	1.94	-5.26	9.68	0.608
CD62E+ (Activated endothelium)	13 wks	-19.21	-27.51	-9.96	**< 0.001**
	$PM_{2.5}$				
	Day 0	1.64	-3.67	7.24	0.552
	Day -1	7.01	0.36	14.11	**0.039**
	1 wk	4.52	-5.33	15.39	0.382
	13 wks	-24.68	-35.18	-12.48	**< 0.001**
	PM_{10}				
	Day 0	0.28	-3.46	4.16	0.886
	Day -1	4.23	-0.05	8.70	0.053
	1 wk	-0.05	-6.51	6.85	0.988
CD14+ (macr./monoc.)	13 wks	-12.89	-23.10	-1.31	**0.030**
	$PM_{2.5}$				
	Day 0	-8.15	-16.07	0.52	0.067
	Day -1	10.56	-0.52	22.89	0.063
	1 wk	1.98	-13.71	20.51	0.818
	13 wks	-33.46	-48.97	-13.23	**0.003**

Outcome	Exposure	% change	LCI	UCI	*P-value*
CD25+ (T-reg cells)	**PM_{10}**				
	Day 0	-3.34	-7.30	0.78	0.112
	Day -1	3.15	-2.04	8.62	0.240
	1 wk	-0.82	-7.85	6.74	0.826
	13 wks	-25.63	-33.00	-17.45	**< 0.001**
	$PM_{2.5}$				
	Day 0	-2.68	-7.73	2.65	0.319
	Day -1	7.89	1.14	15.09	**0.022**
	1 wk	2.40	-7.20	13.00	0.636
	13 wks	-33.36	-42.36	-22.96	**< 0.001**
HLA-g+ (Trophoblasts)	**PM_{10}**				
	Day 0	0.71	-1.85	3.34	0.587
	Day -1	1.45	-1.37	4.36	0.315
	1 wk	0.54	-3.91	5.21	0.815
	13 wks	-9.80	-17.04	-1.92	**0.016**
	$PM_{2.5}$				
	Day 0	-5.66	-10.31	-0.77	**0.025**
	Day -1	4.59	-1.85	11.46	0.167
	1 wk	-5.13	-14.11	4.79	0.300
	13 wks	-29.42	-39.75	-17.31	**< 0.001**
HERV-w+ (syncitin-1)	**PM_{10}**				
	Day 0	15.25	10.38	20.33	**< 0.001**
	Day -1	14.76	9.72	20.03	**< 0.001**
	1 wk	31.78	22.58	41.68	**< 0.001**
	13 wks	27.02	10.48	46.05	**0.001**
	$PM_{2.5}$				
	Day 0	-3.88	-8.69	1.20	0.133
	Day -1	4.29	-2.04	11.04	0.189
	1 wk	-2.35	-11.30	7.51	0.628
	13 wks	-31.06	-40.72	-19.83	**< 0.001**

Results from multivariable negative binomial regression models on the total population (n=518). Associations between both PM concentration and the FC data were adjusted for age, BMI, Smoking habits, season, temperature, humidity, gestational age at sampling. Bold P values underline statistical significance. A Δ% = (exp (β) −1) * 100, percent variation of each evaluated parameters for 10 μg/m^3 increase for the considered pollutants. LCI and UCI = lower and upper confidence interval.

Individual PM level exposure effects on EVs concentration in the pregnant woman subgroup (n=65).

The estimations of air-pollutant concentrations retrieved from personal sampler (PS) devices are considered the gold standard for exposure data collection, as they provide more reliable data on the actual concentration of air-born particles a subject has been in contact with. Therefore, possible associations between PM concentrations and the investigated EV levels were tested in the subgroup composed by 65 pregnant women, which had worn the PS sampler the morning to reach the hospital in order to attend the blood-drawing and the cardiovascular evaluation (T1). PS device allowed the measurement of different diameter-sized PM particles such as: PM_1, $PM_{2.5}$ PM_4, PM_{10}, and the total amount of suspended particles (TSP), for the mean concentrations of 1 hour and 30 minutes before the medical screening.

When we examined the relationship between PM fractions and EV concentration and type, positive associations were found between each considered PM fraction and the Sum of EVs, and the strongest effects were associated to the finest evaluated PM fractions, PM_1 and $PM_{2.5}$ as shown in Table 9.

Conversely, flow-cytometry data did not present any significant links with the mean PM concentrations measured 1 hour and a half before the cardiovascular screening.

Table 9. Associations between PM concentrations obtained from personal sampler and both NTA and flow-cytometry data.

Outcome	Exposure	Δ%	LCI	UCI	*P-value*
		Mean of exposure 1h30 before			
Sum of EVs	PM_1	21.3	10.0	33.7	**0.0001**
	$PM_{2.5}$	11.9	3.9	20.6	**0.002**
	PM_4	7.3	1.2	13.8	**0.012**
	PM_{10}	2.9	0.0	5.8	**0.034**
	TSP	2.4	0.1	4.6	**0.026**
CD61+ (Platelets)	PM_1	18.5	-2.5	44.0	0.089
	$PM_{2.5}$	10.7	-4.8	28.7	0.189
	PM_4	6.6	-5.3	20.0	0.293
	PM_{10}	0.3	-5.7	6.6	0.924
	TSP	-0.2	-4.8	4.7	0.939
CD105+ (Endothelium)	PM_1	11.9	-4.9	31.6	0.176
	$PM_{2.5}$	5.1	-7.2	19.1	0.430
	PM_4	2.7	-6.9	13.3	0.591
	PM_{10}	-0.9	-5.6	4.0	0.702
	TSP	-1.2	-4.8	2.6	0.544
CD62E+ (Activated Endothelium)	PM_1	5.9	-8.7	22.9	0.450
	$PM_{2.5}$	0.4	-10.0	12.2	0.937
	PM_4	-1.2	-9.3	7.6	0.783
	PM_{10}	-1.9	-5.8	2.2	0.361
	TSP	-1.6	-4.7	1.6	0.329
CD14+ (macr./monoc.)	PM_1	14.8	-12.3	50.3	0.307
	$PM_{2.5}$	11.6	-8.1	35.7	0.261
	PM_4	8.6	-6.0	25.4	0.257
	PM_{10}	2.1	-5.0	9.7	0.561
	TSP	1.3	-4.2	7.1	0.644
CD25+ (T-reg cells)	PM_1	15.3	-1.8	35.4	0.081
	$PM_{2.5}$	7.9	-3.8	20.9	0.194
	PM_4	4.8	-3.9	14.2	0.287
	PM_{10}	0.3	-3.9	4.8	0.877
	TSP	0.0	-3.3	3.5	0.986

Outcome	Exposure	Δ%	LCI	UCI	*P-value*
HLA-g+ (Trophoblasts)	PM_1	-5.7	-19.4	10.4	0.470
	$PM_{2.5}$	-3.8	-14.1	7.7	0.503
	PM_4	-2.0	-10.0	6.7	0.641
	PM_{10}	-1.9	-6.0	2.4	0.386
	TSP	-1.8	-5.0	1.5	0.284
HERV-w+ (syncitin-1)	PM_1	16.2	-2.7	38.8	0.099
	$PM_{2.5}$	5.4	-8.1	20.9	0.452
	PM_4	0.7	-9.6	12.2	0.899
	PM_{10}	-1.9	-6.8	3.1	0.452
	TSP	-1.8	-5.6	2.0	0.352

Results from multivariable negative binomial regression models on the subgroup of pregnant women, whom worn the PS device (n=65). Associations between each considered PM fraction concentration and both NTA and FC data were adjusted for age, BMI, Smoking habits, season, temperature, humidity, gestational age at sampling. Bold P values underline statistical significance. A Δ% = (exp (β) −1) * 100, percent variation of each evaluated parameters for 10 μg/m^3 increase for the considered pollutants. LCI and UCI = lower and upper confidence interval.

Individual PM level exposure effects on the screened cardiovascular outcomes in the pregnant women subgroup (n=65).

As pregnancy is known to induce stressful modifications on the cardiovascular system, characterizing pregnant women as a more susceptible population to the effects of particulate pollution, possible associations between PM data retrieved from both FARM models and personal sampler (PS) device, and the cardiovascular outcomes collected from the subgroup composed by 65 pregnant women were tested. Information about diastolic (DP) and systolic (SP) pressure at rest as well as the heart rate (HR) were collected and the results of the applied multivariable regression models are reported in Table 10.

Associations were exclusively observed for both the mean PM_{10} and $PM_{2.5}$ of the day before the cardiovascular screening (Day-1) and measured heart rate values at rest (restHR) (PM_{10}-Day-1, ∆%=2.6%, P 0.031; $PM_{2.5}$-Day-1, ∆%=3.4%, P 0.011).

Table 10. Associations between PM concentrations retrieved from both FAMR models and personal sampler and maternal cardiovascular outcomes

Outcome	Exposure	Δ%	LCI	UCI	*P-value*
	PM_{10}				
	Day 0	0.5	-1.9	2.9	0.673
	Day -1	2.6	0.2	4.9	**0.031**
	1 wk	1.2	-2.1	4.5	0.472
	13 wks	-3.9	-9.2	1.8	0.175
	$PM_{2.5}$				
	Day 0	0.3	-2.6	3.3	0.837
	Day -1	3.4	0.8	6	**0.011**
restHR	1 wk	1.9	-2	6	0.338
	13 wks	-3.7	-10.3	3.3	0.287
	Exposure from PS				
	Mean of exposure				
	1h30				
	PM_1	0.9	-2.5	4.5	0.592
	$PM_{2.5}$	0.7	-1.8	3.3	0.562
	PM_4	0.3	-1.7	2.4	0.738
	PM_{10}	-0.3	-1.3	0.8	0.614
	TSP	-0.3	-1.1	0.6	0.52
	PM_{10}				
	Day 0	0.69	-1.26	2.68	0.48
	Day -1	1.36	-0.72	3.48	0.20
Diastolic Pressure	1 wk	1.85	-1.07	4.86	0.21
	13 wks	-1.86	-6.66	3.19	0.46
	$PM_{2.5}$				
	Day 0	0.35	-1.99	2.74	0.77
	Day -1	1.05	-1.33	3.49	0.38
	1 wk	1.70	-1.86	5.38	0.35
	13 wks	-1.44	-7.38	4.88	0.64
	Exposure from PS				
	Mean of exposure				
	1h30				
	PM_1	1.24	-1.27	3.81	0.33
Diastolic Pressure	$PM_{2.5}$	0.86	-0.98	2.73	0.36
	PM_4	0.31	-1.22	1.86	0.69
	PM_{10}	-0.26	-1.06	0.55	0.52
	TSP	-0.25	-0.87	0.38	0.42

Outcome	Exposure	Δ%	LCI	UCI	*P-value*
	PM_{10}				
	Day 0	0.14	-1.67	1.99	0.88
	Day -1	-0.02	-1.97	1.97	0.99
	1 wk	0.14	-2.58	2.95	0.92
	13 wks	-2.59	-7.08	2.11	0.27
	$PM_{2.5}$				
	Day 0	-0.25	-2.43	1.97	0.82
	Day -1	0.22	-2.01	2.50	0.84
	1 wk	0.67	-2.67	4.13	0.69
Systolic Pressure	13 wks	-2.21	-7.82	3.75	0.45
	Exposure from PS Mean of exposure 1h30				
	PM_1	-0.62	-3.04	1.86	0.61
	$PM_{2.5}$	-0.69	-2.46	1.12	0.44
	PM_4	-0.87	-2.32	0.60	0.24
	PM_{10}	-0.68	-1.43	0.07	0.08
	TSP	-0.54	-1.12	0.05	0.07

Results from multivariate regression models on the subgroup of pregnant women, who worn the PS device (n=65). Associations between each considered PM fraction concentration and cardiovascular data were adjusted for age, BMI, gestational age at sampling. Bold P values underline statistical significance. A Δ% = (exp (β) −1) * 100, percent variation of each evaluated parameters for 10 µg/m^3 increase for the considered pollutants. LCI and UCI = lower and upper confidence interval.

Compositional overview of bacterial nasal microbiota in the pregnant women subgroup (n=65).

Amplicon-based sequencing analysis was performed to characterize the bacterial nasal microbiota (bNM) and the collection of both T0 and T1 samples allowed the investigation of the bNM succession rate between time-points as well as to further test possible effects induced by PM exposure on the analyzed bacterial community. The bNM analysis was conducted on a final number of 130 nasal swab collected at T0 and T1 from the 65 pregnant women and the final dataset was composed by 1,126,612 joined sequences with a median length of 421 bp. Both T0 and T1 bNM were dominated by the Actinobacteria (mean relative abundance T0: 55.7%; T1: 58.3%), Proteobacteria (T0: 23.0%; T1: 21.0%) and Firmicutes (T0: 20.0%; T1: 19.8%) phyla, as showed in Figure 10a. Examining the nasal bacterial community more in detail, 61 genera were identified. Among them, the top 10 represented taxa were identified as *Corynebacterium_1* (T0: 29.1%; T1: 28.1%), *Cutibacterium* (T0: 15.5%; T1: 17.5%), *Lawsonella* (T0: 9.9%; T1: 11.0%), *Moraxella* (T0: 9.8%; T1: 11.1%), *uncultured_Neisseriaceae* (T0: 9.8%; T1: 7.4%), *Dolosigranulum* (T0: 5.6%; T1: 5.2%), *Staphylococcus* (T0: 5.1%; T1: 5.3%), *Peptoniphilus* (T0: 2.8%; T1: 2.8%), *Anaerococcus* (T0: 2.6%: T1: 2.8%) and *Streptococcus* (T0:1.2%; T1: 1.4%) genera (Figure 10b).

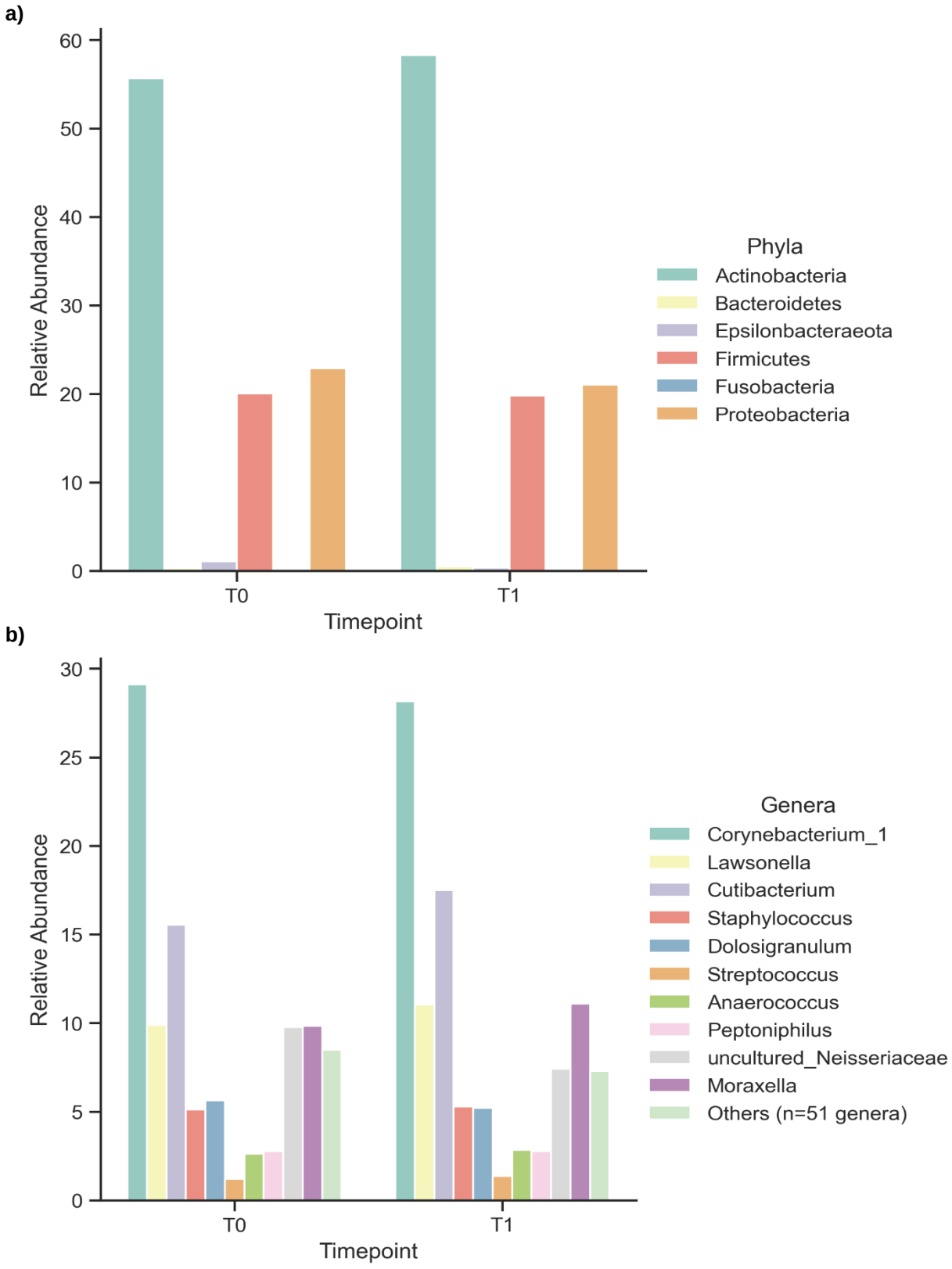

Figure 10. Bar chart showing the mean relative abundance of the bNM structure during T0 and T1; a) average phyla relative abundance in the T0 and T1 samples; b) average top 10 genera relative abundance in T0 and T1 samples.

As mean relative abundance of the identified genera is often referred as imprecise to properly describe the 16S data composition taxa distribution was further investigated in all the analyzed samples at T0 and T1. The result confirmed that *Coryebacterium_1* was the most represented taxa in both time points (prevalence, median relative abundance, Q1-Q3 T0: n=64, 6.4%, 11.3%-41.0%; T1: n=65, 23.6%, 11.1%-40.2%), followed by *Lawsonella* (T0: n=64, 12.6%, 6.1%-25.4%; T1: n=65, 12.2%, 5.9%-26.5%), *Cutibacterium* (T0: n=63, 7.1%, 1.2%-15.0%; T1: n=64, 6.3%, 1.3%-16.4%), *Staphylococcus* (T0: n=64, 4%, 2.1%-7.3%; T1: n=65, 3.4%, 1.4%-7.1%), *Peptoniphilus* (T0: n=61, 1.5%, 0.3%-3.7%; T1: n=60, 1.4%, 0.2%-3.7%), *Dolosigranulum* (T0: n=60, 0.87%, 5.7^{-3}%-3.6%; T1: n=58, 1%, 1.1^{-2}%-3.0%), *uncultured_Neisseriaceae* (T0: n=62, 0.6%, 0.2%-1.5%; T1: n=65, 0.5%, 0.2%-2.0%), *Streptococcus* (T0: n=51, 0.3%, 0.3%-1.0%; T1: n=52, 0.3%, 0.4%-0.9%), *Anaerococcus* (T0: n=53, 0.1%, 1^{-2}%-3.6%; T1: n=54, 0.2%, 8.6^{-3}%-4.4%), and *Moraxella* genera (T0: n =46, 0.02%, 0-4.3%; T1: n=50, 0.03%, 4.5^{-3}%-0.8%), as showed in Figure 11.

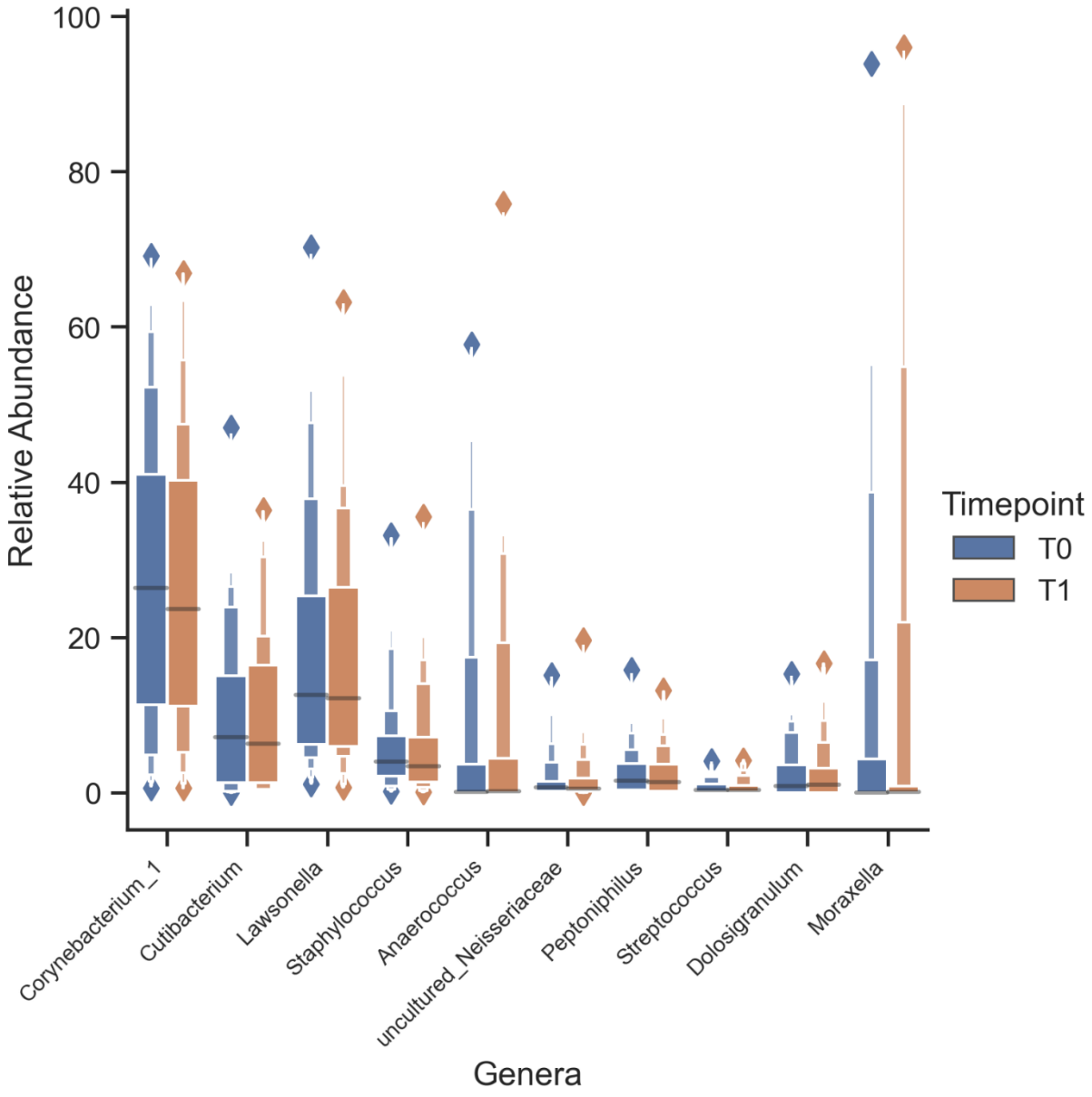

Figure 11. Letter value plot showing the shaping of distribution of the most represented genera in both T0 and T1 specimens. Median value is indicated with a black dash and outliers for each considered taxa are reported as diamond shaped.

Compositional and non-compositional tests were applied considering the most represented genera to verify bNM structural similarity between T0 and T1 samples. Both the tests underlined structural similarity between the identified nasal bacterial taxa between each analyzed time points (P ≥0.05).

Diversity evaluation of the bacterial nasal microbiota in the pregnant women subgroup (n=65)

Alpha and beta diversity analysis were performed to describe bNM diversity features. The rarefaction curves showed that the chosen maximum rarefaction depth (2000 reads) was near to saturation and thus including most of the bNM information found in the processed samples (Figure 12).

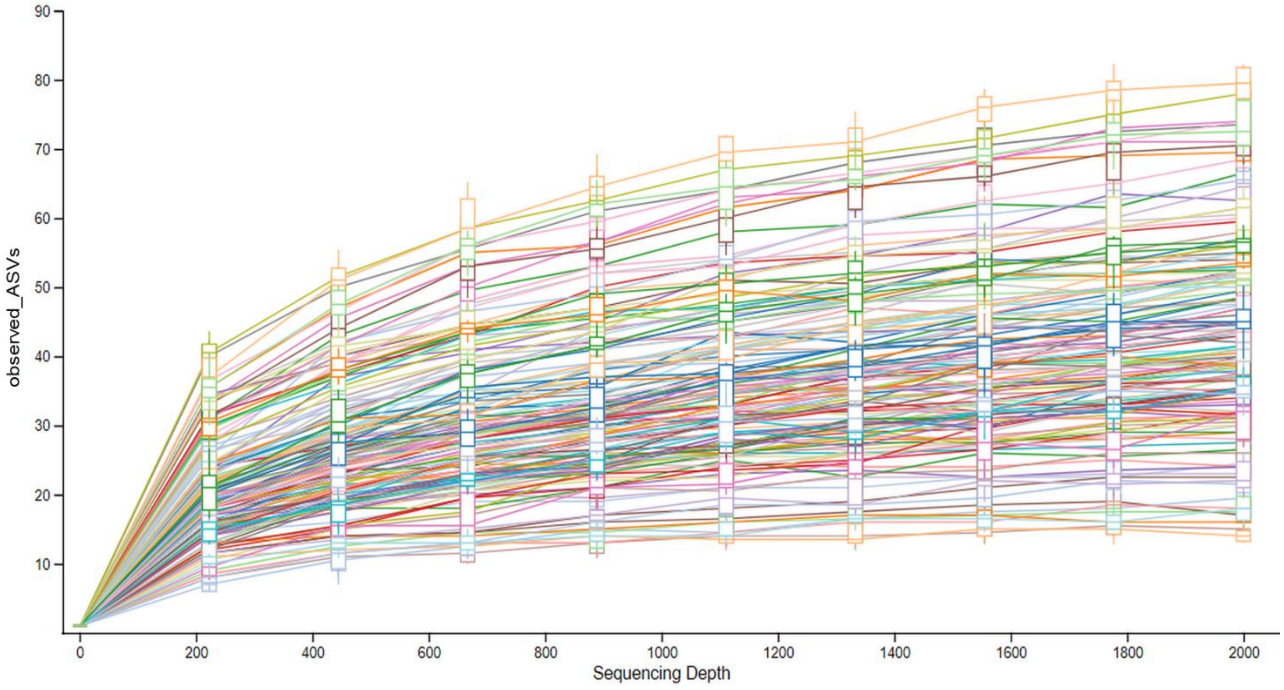

Figure 12. Rarefaction curves generate with the observed_ASVs diversity index in both T0 and T1 (n = 65 per group). The sequencing depth represents the number of sequences, which were clustered into amplicon sequence variants (ASVs).

Alpha-diversity analysis was applied to investigate the diversity feature within the collected sample through the Shannon, observed_ASVs (Obs_ASVs) and Faith's phylogenetic diversity (Faith_pd) indices, providing information about the evenness, richness and phylogenetic features of the inspected bacterial community, respectively. Statistical analysis performed on the selected diversity indices pointed out that the bNM of the enrolled pregnant women on both T0 and T1 did not present any differences in terms of evenness,

phylogenetic and richness features (P ≥ 0.05), as illustrated in Figure 13. Medians, Q1-Q3 and p-value for the tested indices are shown in Table 11.

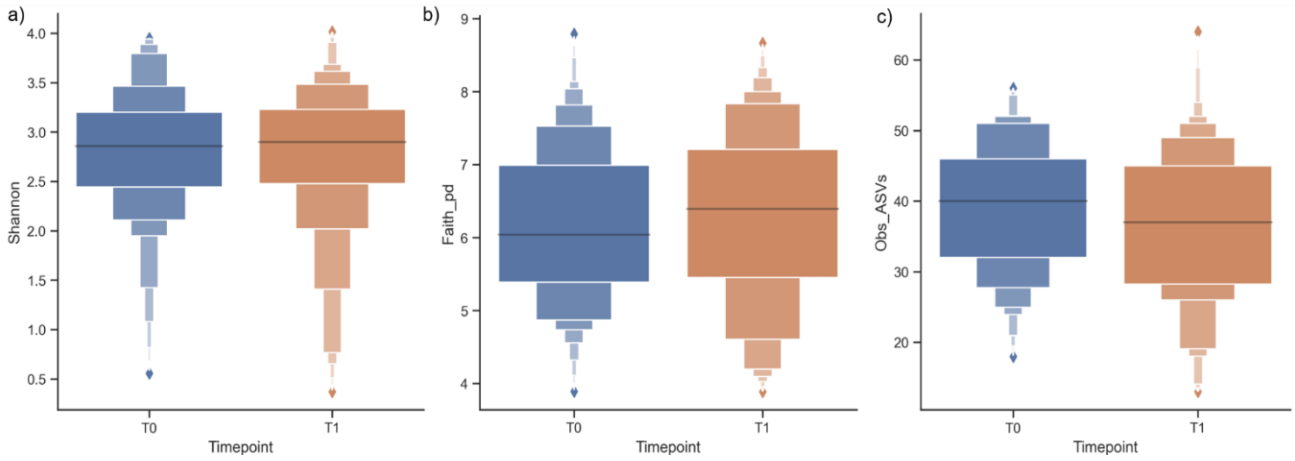

Figure 13. Letter value plot showing the shaping of distribution retrieved values of the applied diversity indices in both T0 and T1 sample. Median value is indicated with a black dash and outliers for each considered taxa are reported as diamond shaped. a) Shannon index, b) Faith's phylogenetic diversity (Faith_pd), c) Observed_ASVs (Obs_ASVs).

Table 11. Alpha diversity medians, Q1-Q3 and p-values for each evaluated index in T0 and T1 samples**.**

		T0		T1		
	Diversity index	**Median**	**Q1-Q3**	**Median**	**Q1-Q3**	***P-value***
a)	Shannon	2.9	2.4-3.2	2.9	2.5-3.2	0.8
b)	Observed_ASVs	40	32-46	37	28-45	0.3
c)	Faith_pd	6	5.4-7	6.4	5.5-7.2	0.5

Beta diversity values were then calculated applying the Weighted_Normalized UniFrac metric to compare and analyze the composition of the bacterial communities between T0 and T1 groups. A PCoA plot was generated, showing that the principal components (PC) 1 and 2 explained 37.95% and 15.85% of the variance between T0 and T1 nasal bacterial communities, when both bacterial presence and abundance as well as phylogenetic diversity

were considered as showed in Figure 14. Analysis of similarity (PERMANOVA) based on the Weighted Normalized UniFrac distance (R-value = 0.12, P ≥ 0.05) showed no separation between T0 and T1 samples, suggesting that no differences in bNM was identified, consistently with the statistical results obtained for taxonomical and alpha diversity analysis.

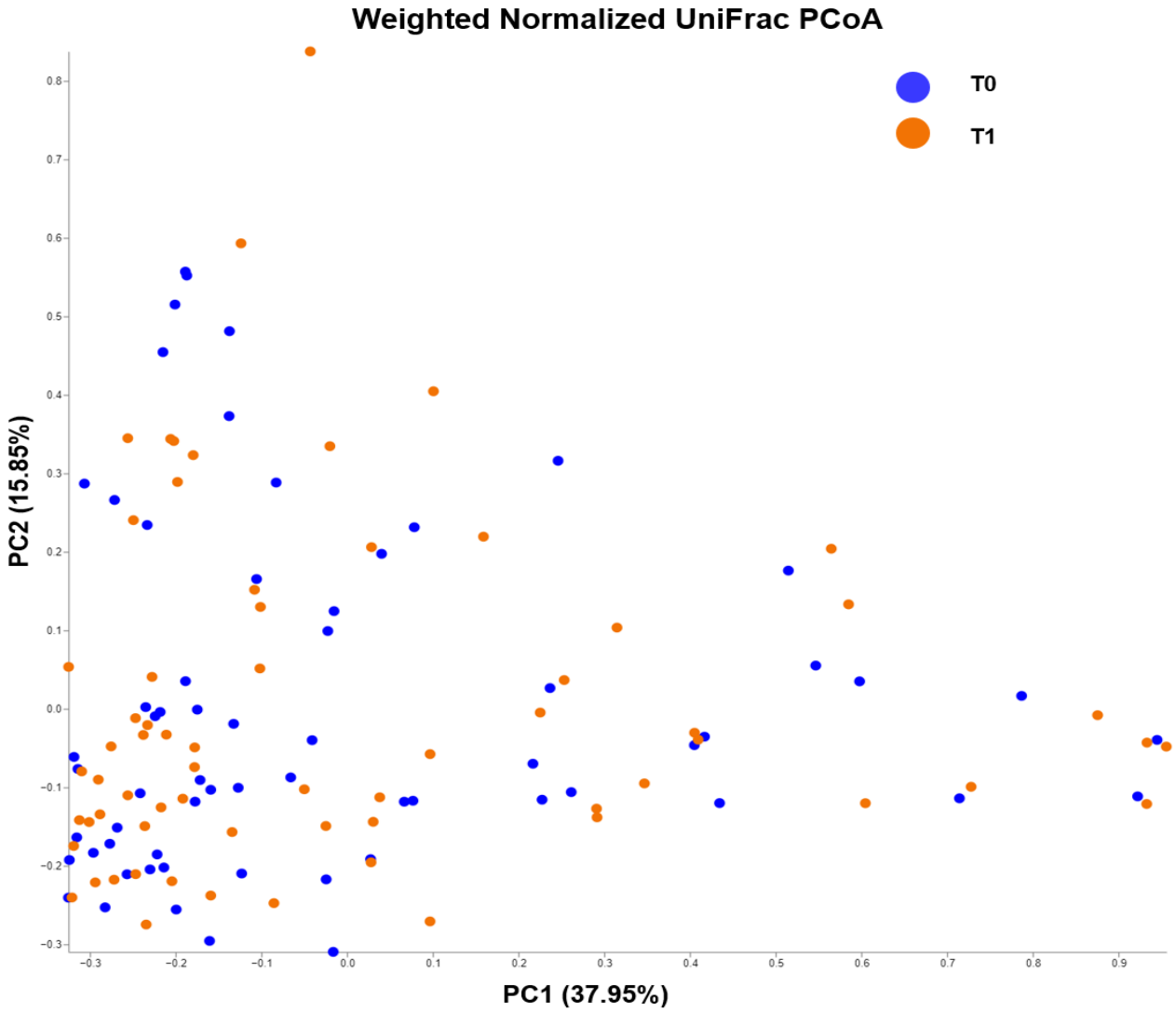

Figure 14. Principal coordinate analysis (PCoA) plot of the similarities between the T0 and T1 groups derived based on Weighted Normalized UniFrac distance. Samples collected at T0 and T1 were colored in blue and orange, respectively.

Individual PM exposure effects on nasal bacterial membership of the pregnant women subgroup (n=65).

PM data derived from both FARM models and PS device were further inspected to verify possible associations with the bacterial nasal community features observed in the subgroup of 65 pregnant women.

No significant associations were identified between the tested air-pollutant concentrations and bNM variations in terms of either richness, evenness or phylogenetic diversity (P ≥0.05). However, the ratio between the evenness and phylogenetic diversity bNM characteristics (Shannon-Faith_pd ratio) showed to be negatively linked to the mean PM_1 levels collected by PS device 1h30 before the cardiovascular evaluation (β*10= -0.03, P 0.029) and a similar trend was observed also for $PM_{2.5}$ fraction (β*10= -0.02, P 0.061), as reported in Table 12.

Table 12. Associations between PM concentrations retrieved from both FARM models and personal sample on alpha-diversity index values

Alpha diversity index	Exposure	β x 10	LCI	UCI	*P-value*
Faith pd	**PM_{10}**				
	Day 0	0.00	-0.17	0.17	0.993
	Day -1	-0.04	-0.22	0.14	0.653
	1 wk	-0.10	-0.34	0.15	0.430
	13 wks	-0.30	-0.72	0.13	0.166
	$PM_{2.5}$				
	Day 0	-0.03	-0.24	0.18	0.790
	Day -1	-0.03	-0.23	0.17	0.763
	1 wk	-0.14	-0.44	0.16	0.355
	13 wks	-0.42	-0.94	0.10	0.108
Observed ASVs	**PM_{10}**				
	Day 0	0.09	-1.41	1.60	0.902
	Day -1	0.08	-1.49	1.64	0.922
	1 wk	-0.72	-2.88	1.43	0.504
	13 wks	-2.73	-6.41	0.95	0.142
	$PM_{2.5}$				
	Day 0	-0.09	-1.93	1.74	0.920
	Day -1	0.34	-1.42	2.11	0.699
	1 wk	-0.87	-3.48	1.75	0.511
	13 wks	-3.66	-8.17	0.85	0.110
Shannon	**PM_{10}**				
	Day 0	-0.03	-0.14	0.08	0.590
	Day -1	0.03	-0.08	0.14	0.586
	1 wk	-0.05	-0.20	0.11	0.546
	13 wks	-0.02	-0.28	0.25	0.900
	$PM_{2.5}$				
	Day 0	-0.04	-0.17	0.09	0.578
	Day -1	0.04	-0.08	0.17	0.523
	1 wk	-0.05	-0.24	0.14	0.598
	13 wks	-0.03	-0.36	0.29	0.843
Shannon-Faith_pd ratio	**PM_{10}**				
	Day 0	-0.01	-0.03	0.01	0.195
	Day -1	0.00	-0.02	0.02	0.714
	1 wk	-0.01	-0.03	0.02	0.533
	13 wks	0.02	-0.03	0.06	0.427
	$PM_{2.5}$				
	Day 0	-0.01	-0.03	0.01	0.252
	Day -1	0.00	-0.02	0.03	0.685
	1 wk	-0.01	-0.04	0.02	0.666
	13 wks	0.03	-0.03	0.08	0.343

Alpha diversity index	Exposure	β x 10	LCI	UCI	*P-value*
	Mean of exposure 1h30 before				
Faith pd	PM_1	-0.009	-0.250	0.233	0.942
	PM_{25}	-0.020	-0.195	0.156	0.823
	PM_4	-0.022	-0.166	0.121	0.755
	PM_{10}	0.012	-0.062	0.086	0.741
	TSP	0.017	-0.040	0.075	0.550
Observed_ASVs	PM_1	0.01	-2.15	2.16	0.996
	PM_{25}	0.01	-1.56	1.57	0.990
	PM_4	-0.05	-1.33	1.23	0.937
	PM_{10}	0.15	-0.50	0.81	0.639
	TSP	0.18	-0.33	0.69	0.489
Shannon	PM_1	-0.11	-0.25	0.02	0.104
	$PM_{2.5}$	-0.08	-0.18	0.02	0.133
	PM_4	-0.06	-0.14	0.03	0.172
	PM_{10}	-0.02	-0.07	0.02	0.293
	TSP	-0.02	-0.05	0.02	0.338
Shannon-Faith_pd ratio	PM_1	-0.03	-0.05	-0.003	**0.029**
	$PM_{2..5}$	-0.02	-0.03	0.00	0.061
	PM_4	-0.01	-0.03	0.00	0.125
	PM_{10}	-0.01	-0.01	0.00	0.143
	TSP	0.00	-0.01	0.00	0.127

Results from multivariate regression models on the subgroup of pregnant women, who worn the PS device (n=65). Associations between each considered PM fraction concentration and each tested diversity index were adjusted for age, BMI, gestational age at sampling. Bold P values underline statistical significance. β*10 value indicates the percentage variation of each evaluated parameters for 10 μg/m^3 increase for the considered pollutants. LCI and UCI = lower and upper confidence interval.

Exposure effects of PM was also evaluated for statistical significance against the structural features observed in the pregnant women bNM, such as the proportion of gram-negative bacteria (% Gram-) as well as the relative abundance (RA) of the most represented bacterial genera.

As reported in Table 13, no significant relationships were identified between all the observed PM concentration and the % Gram- ($P \geq 0.05$).

Table 13. Associations between PM concentrations retrieved from FARM models and personal sampler on the relative frequency of gram-negative bacteria

Outcome	Exposure	β x 10	LCI	UCI	*P-value*
	PM_{10}				
	Day 0	0.03	-0.01	0.07	0.105
	Day -1	0.02	-0.02	0.06	0.415
	1 wk	0.04	-0.01	0.10	0.111
	13 wks	0.03	-0.07	0.12	0.555
% Gram-	**$PM_{2.5}$**				
	Day 0	0.04	-0.01	0.08	0.120
	Day -1	0.02	-0.03	0.06	0.468
	1 wk	0.06	-0.01	0.12	0.088
	13 wks	0.04	-0.08	0.16	0.507
	Mean of exposure 1h30 before				
	PM_1	0.00	-0.05	0.06	0.934
	PM_{25}	0.00	-0.04	0.04	0.839
% Gram-	PM_4	-0.01	-0.04	0.03	0.646
	PM_{10}	-0.01	-0.02	0.01	0.410
	TSP	-0.01	-0.02	0.01	0.286

Results from multivariate regression models on the subgroup of pregnant women, who worn the PS device (n=65). Associations between each considered PM concentration and the percentage of gram-negative sequences found during bNM analysis were adjusted for age, BMI, gestational age at sampling. Bold P values underline statistical significance. β*10 value indicates the percentage variation of each evaluated parameters for 10 μg/m^3 increase for the considered pollutants. LCI and UCI = lower and upper confidence interval.

On the other hand, associations between PM_{10} and $PM_{2.5}$ and the relative abundance of *Corynebacterium* and *Staphylococcus* genera were found. All the identified statistical associations showed a negative direction between the considered exposures and the RA of the significant bacteria (FDR ≤ 0.15), as showed in Table 14.

Table 14. Associations between PM concentrations retrieved from FARM models and the relative abundance of the most represented genera

Genera	Exposure	β x 10	LCI	UCI	*P-value*	FDR
Anaerococcus	**PM_{10}**					
	Day 0	0.00	0.00	0.00	0.687	0.78
	Day -1	0.00	0.00	0.01	**0.044**	0.37
	1 wk	0.00	0.00	0.01	0.401	0.76
	13 wks	0.00	-0.01	0.01	0.593	0.77
	$PM_{2.5}$					
	Day 0	0.00	-0.01	0.00	0.421	0.76
	Day -1	0.00	0.00	0.01	0.083	0.47
	1 wk	0.00	-0.01	0.01	0.633	0.77
	13 wks	-0.01	-0.02	0.01	0.385	0.76
Corynebacterium_1	**PM_{10}**					
	Day 0	-0.03	-0.06	-0.01	**0.020**	**0.11**
	Day -1	-0.02	-0.05	0.00	0.085	0.25
	1 wk	-0.03	-0.07	0.01	0.137	0.29
	13 wks	-0.02	-0.08	0.05	0.627	0.71
	$PM_{2.5}$					
	Day 0	-0.04	-0.07	-0.01	**0.019**	**0.11**
	Day -1	-0.03	-0.06	0.00	0.090	0.25
	1 wk	-0.04	-0.09	0.00	0.059	0.25
	13 wks	-0.03	-0.11	0.06	0.540	0.66
Lawsonella	**PM_{10}**					
	Day 0	0.00	-0.02	0.01	0.822	0.98
	Day -1	0.00	-0.02	0.01	0.865	0.98
	1 wk	-0.01	-0.03	0.01	0.463	0.98
	13 wks	-0.03	-0.07	0.00	0.084	0.48
	$PM_{2.5}$					
	Day 0	0.00	-0.02	0.01	0.709	0.98
	Day -1	0.00	-0.02	0.02	0.978	0.98
	1 wk	-0.01	-0.04	0.01	0.388	0.94
	13 wks	-0.04	-0.09	0.00	0.053	0.45

Genera	Exposure	β x 10	LCI	UCI	*P-value*	FDR
Staphylococcus	**PM_{10}**					
	Day 0	0.00	-0.01	0.01	0.687	0.94
	Day -1	0.00	-0.01	0.01	0.760	0.94
	1 wk	-0.01	-0.02	0.01	0.361	0.94
	13 wks	-0.03	-0.06	-0.01	**0.006**	**0.10**
	$PM_{2.5}$					
	Day 0	0.00	-0.01	0.01	0.942	0.94
	Day -1	0.00	-0.01	0.01	0.858	0.94
	1 wk	0.00	-0.02	0.01	0.587	0.94
	13 wks	-0.04	-0.07	-0.01	**0.014**	**0.12**

Results from multivariate regression models on the subgroup of pregnant women, who worn the PS device (n=65). Associations between each considered PM levels and genera relative abundance bNM analysis were adjusted for age, BMI, gestational age at sampling. Bold FDR values underline statistical significance. β*10 value indicates the percentage variation of each evaluated parameters for 10 μg/m^3 increase for the considered pollutants. LCI and UCI = lower and upper confidence interval.

Individual PM Exposure effects on EV data obtained from nanoparticle tracking analysis in the pregnant women subgroup (n=65) stratified for gram-negative abundance

As bNM inhabits the first compartment of the respiratory tract targeted by air-born particles, associations were investigated between PM concentrations and the EV data obtained using the NTA instrumentation, considering the nasal bacterial community as a possible effect modifier. To do that, the 65 pregnant women were stratified according to their %RA of gram-negative into Gram- ≤ 20% and Gram- > 20% (gram-negative %RA cut-off ≤20% and >20%, respectively).

Descriptive analysis of the distribution of mean vesicle concentrations in both the groups was performed, reporting for each EV size (from 30 to 700 nm) the mean concentration and significance in the enrolled groups, in the upper and lower part of the plot respectively, as showed in Figure 15. In particular, pregnant women characterized by a bNM with a %RA of gram-negative bacteria greater than 20% were characterized by a higher concentration of EVs ranging between 86-119 nm ($P < 0.05$), with a peak at 131 nm as showed in plot below.

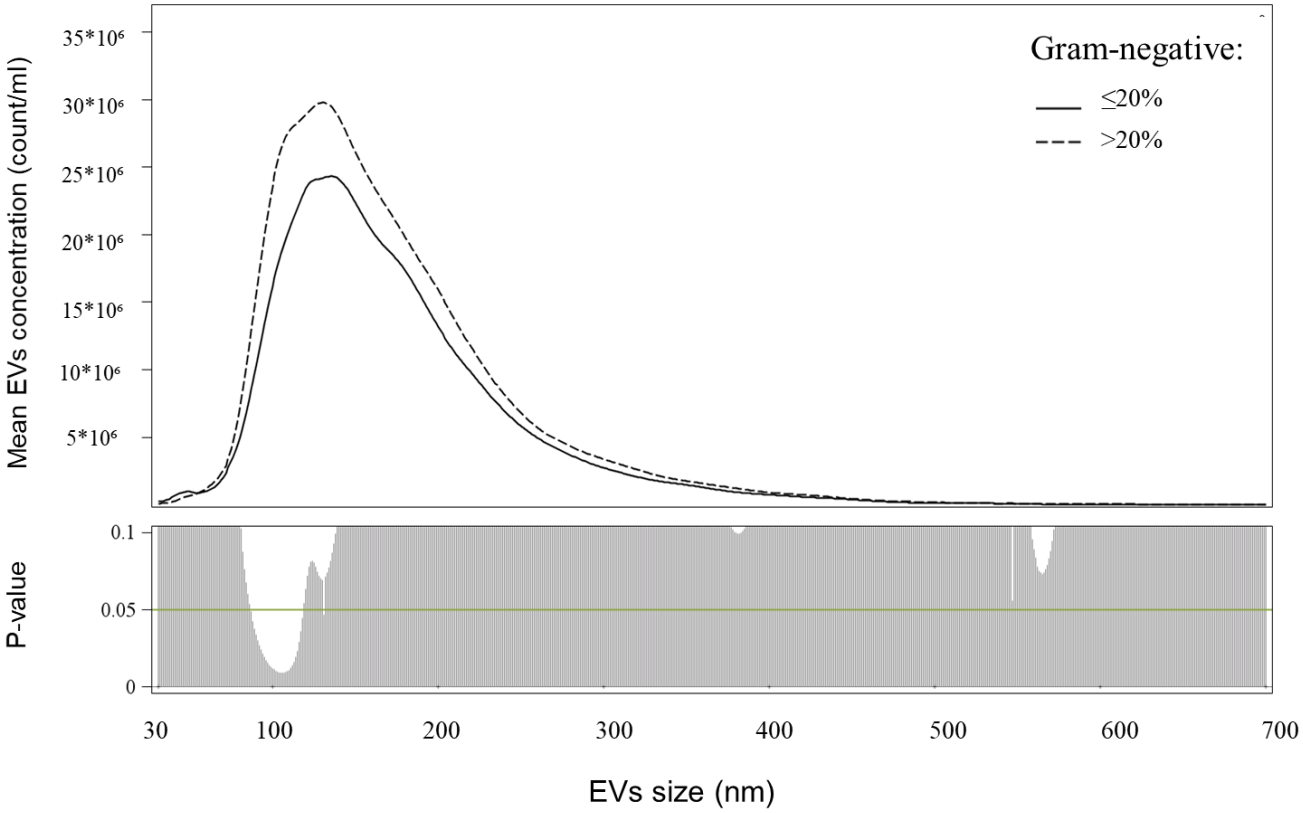

Figure 15. NTA plasma EV size profile. The upper panel of the figure reports EV concentration for each size for Gram- ≤ 20% (solid line) and Gram- > 20% (dashed line) groups. The lower panel reports the p-values of comparisons of each size EV for the entire 30–700 nm size range (Gram- ≤ 20% VS Gram- > 20%).

Moreover, the applied statistical models underlined a opposite behavior between the two considered groups when the associations between the total amount of plasmatic EVs (Sum of EVs) and mean of PM concentration were tested, highlighting positive associations between between both PM_{10} and $PM_{2.5}$ Day 0 exposure and the Sum of EVs for the Gram-negative ≤ 20% group (PM_{10} Day 0: β*10= 0.105, P <0.001; $PM_{2.5}$ Day 0: β*10= 0.144, P 0.004), as showed in Figure 16 and 17.

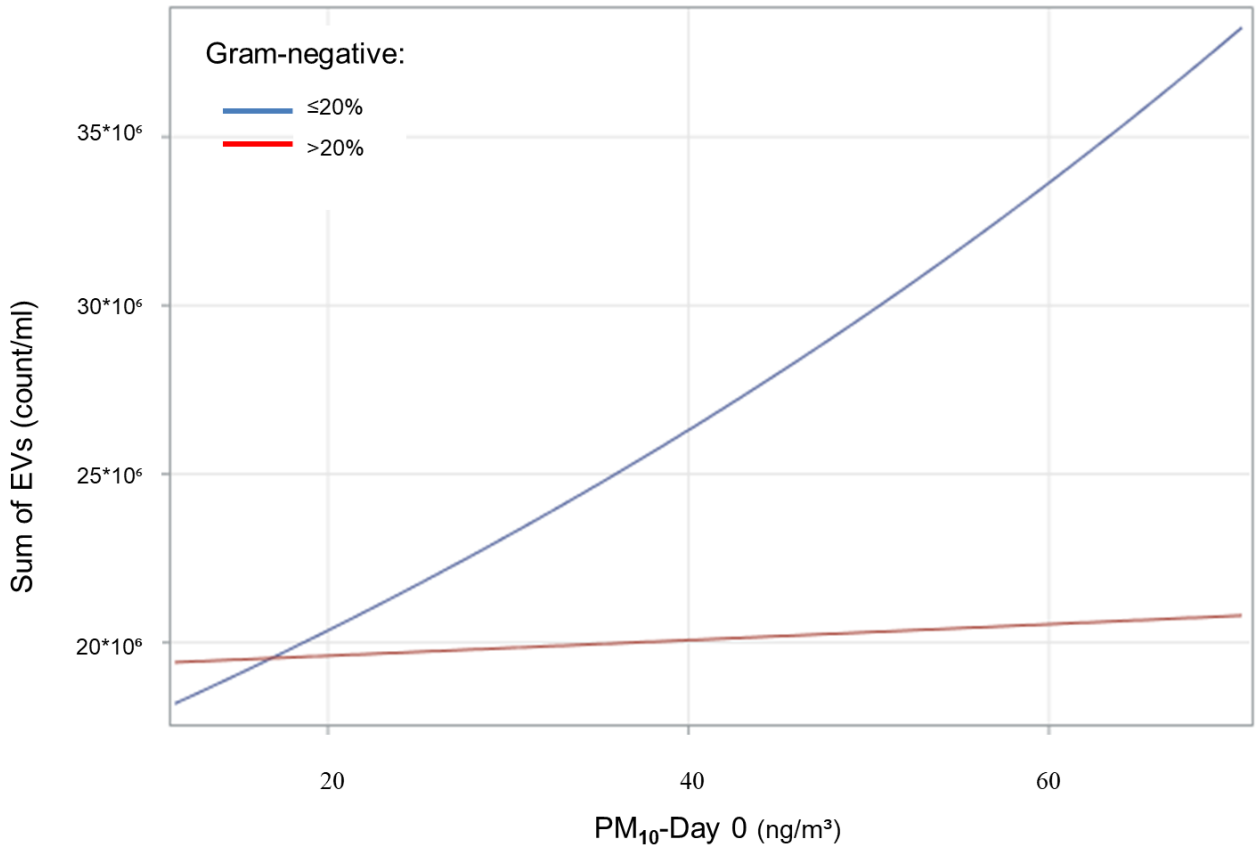

Figure 16. Graphical representation of the multivariable regression model results between mean PM_{10}-Day 0 levels and the total amount of plasmatic EVs (Sum of EVs) obtained from NTA analysis, adjusted for age, BMI, Smoking habits, season, temperature, humidity, gestational age at sampling. Blue and red line belong to the Gram- ≤ 20% and Gram- > 20% groups, respectively.

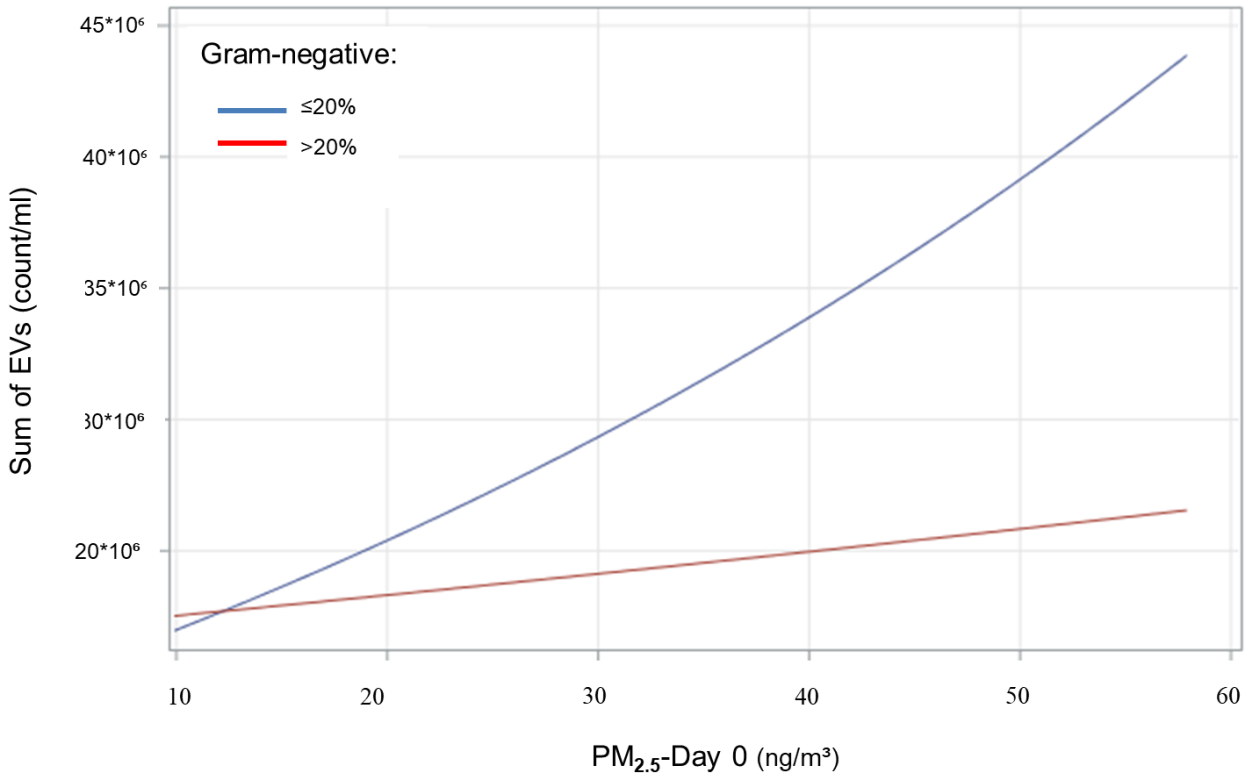

Figure 17. Graphical representation of the multivariable regression model results between mean $PM_{2.5}$-Day 0 levels and the total amount of plasmatic EVs (Sum of EVs) obtained from NTA analysis, adjusted for age, BMI, Smoking habits, season, temperature, humidity, gestational age at sampling. Blue and red line belong to the Gram- ≤ 20% and Gram- > 20% groups, respectively.

DISCUSSION

Exposure to air particulate pollutants is one of the globally leading causes of both the exacerbation and worsening of several adverse conditions, including adverse pregnancy outcomes [1,2]. The mechanisms underlying these effects are still little known.

This study hypothesized that PM exposure, chosen as a paradigmatic environmental stressor, might modify both the EV signaling network and the bNM, leading to an alteration in maternal health and eventually influencing the newborn development.

The available studies, which investigated the relationship between PM exposure and EV production in healthy subjects, support the hypothesis of a positive association that might enhance inflammation [72,74].

This study is the first that examined this association in pregnant women. Pregnancy is characterized by a chronic low-grade inflammation and by the need to keep acute inflammation under strict control. Accordingly, our study showed a consistent negative association between PM_{10} measured at different time lags and number of EVs. This effect is mainly explained by the reduced release of inflammatory cell EVs (CD14+ and CD62E+) in response to PM_{10} (both short and long term). On the other hand, this finding is counterbalanced by the increased production of placenta-derived EVs (HERV-w+), which are known as fine modulators of maternal immune system and have a role in inducing maternal tolerance towards the developing fetus.

As regards $PM_{2.5}$, no clear association was identified in the whole population between exposure and EV production. This result might be partly due to the incompleteness of the $PM_{2.5}$ series, which are only available for a minority of women.

More reliable data on the finest fractions (PM_1, $PM_{2.5}$ and PM_4), are given by personal sampler worn by a subgroup of women for a very short period of time preceding the blood drawing (1.5 hours). As we considered this extremely acute effect, we observed a generalized increment in all the EV subtypes, as well as in the EV count. The possible explanation is that such a short time is not enough to allow the placental EVs to exert their mitigating effect.

The proinflammatory role exerted by CD14+ and CD62E+ EVs has been previously described, in agreement with our hypothesis linking the maternal tolerogenic microenvironment to lowered levels of these EV subtypes after PM_{10}-induced stimuli [112–115]. Indeed, it was published that alveolar macrophages-derived EVs may be implicated in the pathophysiology of acute lung injures in presence of noxious stimuli after the interaction with lung epithelial cells via NF-κB activation through a PPAR-γ-dependent pathway, underling a proinflammatory role for this EV subtype [112–114]. Similarly, the ability of endothelial-derived EVs in triggering inflammatory levels has been seen also after particulate pollutant exposure, as the inhaled PM particles could alter the functionality of these EVs, switching from an anti-inflammatory to a pro-inflammatory phenotype, as stated by Benedikter et al. [115].

The different behavior observed for syncytin-1 positive EVs (HERV-w+), the only tested EV subtype positively associated with each PM_{10} exposure time lag, could be explained by its intrinsic regulatory role, as this particular EV subtype may participate in the establishment of an immune-tolerant microenvironment interacting with specific maternal cells [81,82,116].

On the contrary, the increment of circulating EVs after acute fine PM effects, which have been observed to boost EV release in a dose-dependent manner, could be addressed in the ability of the finest particles to travel into and deposit itself on the surface of the respiratory system inducing high inflammatory reactions, and might thus impair the maternal tolerogenic

state [1,8]. In addition, high levels of plasmatic EVs are generally measured after particulate pollution exposure since both PM- induced inflammation and oxidative stress have been shown to increase the number of circulating vesicles [9,73,117]

The relevance of PM-induced effects on the composition of the bacterial nasal microbiota (bNM) as well as its role as possible effect modifier between air pollution and EV concentrations in healthy subjects have been recently investigated [20,23].

Accordingly, our results indicated, beside bNM structure consistency, a reduction in terms of bNM diversity, through the obtained negative association between acute PM_1 exposure and the Shannon/Faith_pd index ratio. This effect could be partially attributable to the reduction of two of the most represented bacterial genera after PM exposure: *Staphylococcus spp.* and *Corynebacterium spp.* Decrements in terms of respiratory commensal bacteria and diversity have been linked to either adverse conditions or stressor stimuli [20–22,97], however the stability observed between the bNM composition at both T0 and T1 might suggest that the pregnancy-induced tolerogenic state could help to keep intact the indigenous bNM structure and in turn stop the overgrowth of pathobionts after PM stimuli.

Moreover, concordant results were found with our previous study involving heathy subjects, which suggested a possible contribution of a balanced bNM in mediate PM exposure effects in terms of plasmatic EV concentrations, as found for the Gram- ≤20% group [23]. On the contrary, the lack of association between PM exposure and EV levels for the Gram- > 20% group could be explained by a more unevenly distributed bNM as well as to a higher basal concentrations of EVs, possible indicators of an enhanced inflammatory environment and an already saturated response-mechanism to PM stimuli in term of secreted EVs, respectively.

Along with the induced tolerogenic state, several anatomical and physiological changes are observed during gestation also within the cardiovascular system, characterizing pregnant women as a susceptible population to PM effects.

The link between PM levels and adverse cardiovascular outcomes is well-documented in the literature, and the negative effects of particulate pollutant exposure have been also described during pregnancy [1,3,8,44,46,47,118].

Consistently, an association between PM_{10} and $PM_{2.5}$ exposures measured the day before the blood drawing (Day-1) and the heart rate (HR) was identified.

Since pregnant women may have different susceptibility to air pollution effects from non-pregnant subjects, the obtained associations cannot be easily equalized to the results found in the literature, as discrepant conclusions have been found in epidemiological studies between short-term PM levels and HR values as reported by Breitner et al [119]. However, our data could suggest that short-term PM exposure during pregnancy may alter the cardiovascular compensatory mechanism, in this case evaluated as increments in the heart rate, crucial to counteract PM induced changes in blood pressure, which was found to be heightened by the exposure to air pollutants during the 1st trimester of gestation [120].

Considering the whole study population, birth weight and gestational age were investigated as these newborn outcomes have already been associated by previous studies with the negative effect of air pollutants, as strong predictors of both short and long term prognosis of infants [60,121]. Consistently, although no associations were identified when the weight at birth was tested, the levels of PM measured either during the second trimester (2nd trimester) or throughout the whole pregnancy (all pregnancy) were associated with a reduction of the gestational age at birth.

This effect could be explained by both PM-induced oxidative stress and inflammatory reactions that in turn might impair the proper fetal development. In agreement with the observed results, maternal exposure to $PM_{2.5}$ levels during either the 2nd trimester or the whole pregnancy were found to positively correlate with the risk for a SGA fetus and consequently heightening the risk of adverse outcomes in the later life [7,57,122]. Moreover, same evidences have been found as well for PM_{10} concentrations, may thus underlining this pregnancy stage as more susceptible to exposure to PM particles in terms of SGA risk [58,59].

The lack of associations observed between PM exposure and the weight at birth, which are often described in the literature to negatively correlate with PM_{10} and $PM_{2.5}$ concentrations [7,56], could be due to either methodological and slightly biological differences in the recruited population or to different composition of inhaled particulate pollutants, thus affecting inducing a different degree of damages, as probably for blood pressure outcomes.

To our knowledge, this is the first study aimed to enlighten the role of bNM and the EV cross-talk in determining the effects of PM exposure levels on healthy pregnancies as well as on newborn outcomes. The discussed and above described results were obtained from a wide and well characterized population composed by 518 pregnant women, which consequently yielded sufficient statistical power. The novelty of this project is also settled in the investigation of the bNM as possible effect modifier between PM exposure and EV levels.

This project has also three major drawbacks. The evaluation of air pollutant effects applying data derived from models has been often referred as imprecise to properly assess biological modifications induced by PM concentration, as they could lead to exposure misclassifications. However, the assessed consistency between FARM models and PS data, especially for the obtained EVs results, suggest the reliability of the observed findings and the possibility to integrate these data.

Second, the results obtained for the 65 of pregnant women may are not enough to cover the intrinsic bNM variations as well to yield a proper statistical power. Nonetheless, the consistency with previous studies make us confident that they are not due to chance. Third, the modifications induced by PM concentrations on the amount of plasmatic EVs could be addressed, in addition to the bNM, to other microbiota compartments, such as the gastrointestinal one. However, since this study aimed to assess how the microbiota modifies the variation of plasmatic EVs induced by PM exposure, the attention was focused on the bacterial nasal community, which is considered as the first target of PM inhaled particles.

CONCLUSIONS

Our findings contribute to shed light on the possible role exerted by both EV concentration and the bNM in pregnant women in mediating the effects of PM exposure either spread through the body or focused on the first part of the upper respiratory tract, in terms of EV and bNM variations respectively.

Besides the well-documented effects of air pollution exposure during pregnancy, additional studies are needed with the purpose of obtaining, for example, a deeper insight into EV content. Moreover, a comprehensive characterization of the bNM components is necessary to better clarify the relationship between the host and the bacterial nasal community and how it could react to air pollution exposure, especially during gestation.

REFERENCES

1. Kim KH, Kabir E, Kabir S. A review on the human health impact of airborne particulate matter. Environ. Int. 2015.

2. Winckelmans E, Cox B, Martens E, Fierens F, Nemery B, Nawrot TS. Fetal growth and maternal exposure to particulate air pollution More marked effects at lower exposure and modification by gestational duration. Environ Res. 2015;

3. Sun M, Yan W, Fang K, Chen D, Liu J, Chen Y, et al. The correlation between PM2.5 exposure and hypertensive disorders in pregnancy: A Meta-analysis. Sci Total Environ. 2020;

4. Melchiorre K, Thilaganathan B, Giorgione V, Ridder A, Memmo A, Khalil A. Hypertensive Disorders of Pregnancy and Future Cardiovascular Health. Front Cardiovasc Med. 2020;

5. Scharf RJ, Stroustrup A, Conaway MR, Deboer MD. Growth and development in children born very low birthweight. Arch Dis Child Fetal Neonatal Ed. 2016;

6. Schlaudecker EP, Munoz FM, Bardají A, Boghossian NS, Khalil A, Mousa H, et al. Small for gestational age: Case definition & guidelines for data collection, analysis, and presentation of maternal immunisation safety data. Vaccine. 2017.

7. Yuan L, Zhang Y, Gao Y, Tian Y. Maternal fine particulate matter (PM 2.5) exposure and adverse birth outcomes: an updated systematic review based on cohort studies. Environ. Sci. Pollut. Res. 2019.

8. Alemayehu YA, Asfaw SL, Terfie TA. Exposure to urban particulate matter and its association with human health risks. Environ. Sci. Pollut. Res. 2020.

9. Neven KY, Nawrot TS, Bollati V. Extracellular Vesicles: How the External and Internal Environment Can Shape Cell-To-Cell Communication. Curr. Environ. Heal. reports. 2017.

10. Alkoussa S, Hulo S, Courcot D, Billet S, Martin PJ. Extracellular vesicles as actors in the air pollution related cardiopulmonary diseases. Crit. Rev. Toxicol. 2020.

11. Van Niel G, D'Angelo G, Raposo G. Shedding light on the cell biology of extracellular vesicles. Nat. Rev. Mol. Cell Biol. 2018.

12. Skog J, Würdinger T, van Rijn S, Meijer DH, Gainche L, Curry WT, et al. Glioblastoma microvesicles transport RNA and proteins that promote tumour growth and provide diagnostic biomarkers. Nat Cell Biol. 2008;

13. Hunter MP, Ismail N, Zhang X, Aguda BD, Lee EJ, Yu L, et al. Detection of microRNA expression in human peripheral blood microvesicles. PLoS One. 2008;

14. Johnson BL, Iii, Kuethe JW, Caldwell CC. Neutrophil derived microvesicles: emerging role of a key mediator to the immune response. Endocr Metab Immune Disord Drug Targets. 2014;

15. Zhang J, Li H, Fan B, Xu W, Zhang X. Extracellular vesicles in normal pregnancy and pregnancy-related diseases. J. Cell. Mol. Med. 2020.

16. Gill M, Motta-Mejia C, Kandzija N, Cooke W, Zhang W, Cerdeira AS, et al. Placental syncytiotrophoblast-derived extracellular vesicles carry active NEP (Neprilysin) and are increased in preeclampsia. Hypertension. 2019;

17. Tannetta DS, Dragovic RA, Gardiner C, Redman CW, Sargent IL. Characterisation of Syncytiotrophoblast Vesicles in Normal Pregnancy and Pre-Eclampsia: Expression of Flt-1 and Endoglin. PLoS One. 2013;

18. Knight R, Callewaert C, Marotz C, Hyde ER, Debelius JW, McDonald D, et al. The Microbiome and Human Biology. Annu Rev Genomics Hum Genet. 2017;

19. Man WH, De Steenhuijsen Piters WAA, Bogaert D. The microbiota of the respiratory tract: Gatekeeper to respiratory health. Nat. Rev. Microbiol. 2017.

20. Mariani J, Favero C, Spinazzè A, Cavallo DM, Carugno M, Motta V, et al. Short-term particulate matter exposure influences nasal microbiota in a population of healthy subjects. Environ Res. 2018;162.

21. Kumpitsch C, Koskinen K, Schöpf V, Moissl-Eichinger C. The microbiome of the upper respiratory tract in health and disease. BMC Biol. 2019.

22. Hoggard M, Biswas K, Zoing M, Wagner Mackenzie B, Taylor MW, Douglas RG. Evidence of microbiota dysbiosis in chronic rhinosinusitis. Int Forum Allergy Rhinol. 2017;

23. Mariani J, Favero C, Carugno M, Pergoli L, Ferrari L, Bonzini M, et al. Nasal microbiota modifies the effects of particulate air pollution on plasma extracellular vesicles. Int J Environ Res Public Health. 2020;

24. Häggström M. Medical gallery of Mikael Häggström 2014. WikiJournal Med. 2014;

25. Till SR, Everetts D, Haas DM. Incentives for increasing prenatal care use by women in order to improve maternal and neonatal outcomes. Cochrane Database Syst. Rev. 2015.

26. Smith GCS, Shah I, Crossley JA, Aitken DA, Pell JP, Nelson SM, et al. Pregnancy-associated plasma protein A and alpha-fetoprotein and prediction of adverse perinatal outcome. Obstet Gynecol. 2006;

27. Betz D, Fane K. Human Chorionic Gonadotropin. StatPearl; 2020.

28. Sagi-Dain L, Peleg A, Sagi S. First-Trimester Crown-Rump Length and Risk of Chromosomal Aberrations-A Systematic Review and Meta-analysis. Obstet. Gynecol. Surv. 2017.

29. Souka AP, Von Kaisenberg CS, Hyett JA, Sonek JD, Nicolaides KH. Increased nuchal translucency with normal karyotype. Am J Obstet Gynecol. 2005.

30. Oztekin D, Oztekin O, Aydal FI, Tinar S, Adibelli ZH. Embryonic heart rate as a prognostic factor for chromosomal abnormalities. J Ultrasound Med. 2009;

31. Seravalli V, Miller JL, Block-Abraham D, Baschat AA. Ductus venosus Doppler in the assessment of fetal cardiovascular health: An updated practical approach. Acta Obstet. Gynecol. Scand. 2016.

32. Khong SL, Kane SC, Brennecke SP, Da Silva Costa F. First-trimester uterine artery doppler analysis in the prediction of later pregnancy complications. Dis Markers. 2015;

33. Struijk PC, Mathews VJ, Loupas T, Stewart PA, Clark EB, Steegers EAP, et al. Blood pressure estimation in the human fetal descending aorta. Ultrasound Obstet Gynecol. 2008;

34. Huppertz B. The anatomy of the normal placenta. J. Clin. Pathol. 2008.

35. Boss AL, Chamley LW, James JL. Placental formation in early pregnancy: How is the centre of the placenta made? Hum Reprod Update. 2018;

36. Shagana JA, Dhanraj M, Jain AR, Nirosa T. Physiological changes in pregnancy. Drug Invent. Today. 2018.

37. Soma-Pillay P, Nelson-Piercy C, Tolppanen H, Mebazaa A. Physiological changes in pregnancy. Cardiovasc J Afr. 2016;

38. Jørgensen N, Persson G, Hviid TVF. The tolerogenic function of regulatory T cells in pregnancy and cancer. Front. Immunol. 2019.

39. Bai W, Li Y, Niu Y, Ding Y, Yu X, Zhu B, et al. Association between ambient air pollution and pregnancy complications: A systematic review and meta-analysis of cohort studies. Environ. Res. 2020.

40. Stanaway JD, Afshin A, Gakidou E, Lim SS, Abate D, Abate KH, et al. Global, regional, and national comparative risk assessment of 84 behavioural, environmental and occupational, and metabolic risks or clusters of risks for 195 countries and territories, 1990-2017: A systematic analysis for the Global Burden of Disease Stu. Lancet. 2018;

41. World Health Organization. Health Effects of Particulate Matter: Policy implications for countries in eastern Europe, Caucasus and central Asia. J Korean Med Assoc. 2013;

42. Burnett RT, Arden Pope C, Ezzati M, Olives C, Lim SS, Mehta S, et al. An integrated risk function for estimating the global burden of disease attributable to ambient fine particulate matter exposure. Environ Health Perspect. 2014;

43. World Health Organization. Ambient Air Pollution: A global assessment of exposure and burden of disease. World Heal. Organ. 2016.

44. Chen R, Hu B, Liu Y, Xu J, Yang G, Xu D, et al. Beyond PM2.5: The role of ultrafine particles on adverse health effects of air pollution. Biochim Biophys Acta - Gen Subj. 2016;

45. Jia YY, Wang Q, Liu T. Toxicity research of PM2.5 compositions in vitro. Int. J. Environ. Res. Public Health. 2017.

46. Orellano P, Reynoso J, Quaranta N, Bardach A, Ciapponi A. Short-term exposure to particulate matter (PM10 and PM2.5), nitrogen dioxide (NO2), and ozone (O3) and all-cause and cause-specific mortality: Systematic review and meta-analysis. Environ. Int. 2020.

47. Arias-Pérez RD, Taborda NA, Gómez DM, Narvaez JF, Porras J, Hernandez JC. Inflammatory effects of particulate matter air pollution. Environ. Sci. Pollut. Res. 2020.

48. Van Den Hooven EH, De Kluizenaar Y, Pierik FH, Hofman A, Van Ratingen SW, Zandveld PYJ, et al. Air pollution, blood pressure, and the risk of hypertensive complications during pregnancy: The generation r study. Hypertension. 2011;

49. An Z, Jin Y, Li J, Li W, Wu W. Impact of Particulate Air Pollution on Cardiovascular Health. Curr. Allergy Asthma Rep. 2018.

50. Miller MJ, Butler P, Gilchriest J, Taylor A, Lutgendorf MA. Implementation of a standardized nurse initiated protocol to manage severe hypertension in pregnancy. J Matern Neonatal Med. 2020;

51. Brown JM, Harris G, Pantea C, Hwang SA, Talbot TO. Linking air pollution data and adverse birth outcomes: Environmental public health tracking in New York State. J Public Heal Manag Pract. 2015;

52. Westergaard N, Gehring U, Slama R, Pedersen M. Ambient air pollution and low birth weight - are some women more vulnerable than others? Environ. Int. 2017.

53. Yadav S, Rustogi D. Small for gestational age: Growth and puberty issues. Indian Pediatr. 2015.

54. Lawlor DA, Ronalds G, Clark H, Smith GD, Leon DA. Birth weight is inversely associated with incident coronary heart disease and stroke among individuals born in the 1950s: Findings from the Aberdeen children of the 1950s prospective cohort study. Circulation. 2005;

55. Oudgenoeg-Paz O, Mulder H, Jongmans MJ, van der Ham IJM, Van der Stigchel S. The link between motor and cognitive development in children born preterm and/or with low birth weight: A review of current evidence. Neurosci. Biobehav. Rev. 2017.

56. Kumar N. Uncertainty in the relationship between criteria pollutants and low birth weight in Chicago. Atmos Environ. 2012;

57. Stieb DM, Chen L, Beckerman BS, Jerrett M, Crouse DL, Omariba DWR, et al. Associations of pregnancy outcomes and PM2.5 in a national Canadian study. Environ Health Perspect. 2016;

58. Hannam K, McNamee R, Baker P, Sibley C, Agius R. Air pollution exposure and adverse pregnancy outcomes in a large UK birth cohort: Use of a novel Spatio-Temporal modelling technique. Scand J Work Environ Heal. 2014;

59. Symanski E, Davila M, McHugh MK, Waller DK, Zhang X, Lai D. Maternal exposure to fine particulate pollution during narrow gestational periods and newborn health in harris county, Texas. Matern Child Health J. 2014;

60. Pereira G, Bracken MB, Bell ML. Particulate air pollution, fetal growth and gestational length: The influence of residential mobility in pregnancy. Environ Res. 2016;

61. Vinikoor-Imler LC, Davis JA, Meyer RE, Messer LC, Luben TJ. Associations between prenatal exposure

to air pollution, small for gestational age, and term low birthweight in a state-wide birth cohort. Environ Res. 2014;

62. Colombo M, Raposo G, Théry C. Biogenesis, secretion, and intercellular interactions of exosomes and other extracellular vesicles. Annu. Rev. Cell Dev. Biol. 2014.

63. Anthony DF, Shiels PG. Exploiting paracrine mechanisms of tissue regeneration to repair damaged organs. Transplant. Res. 2013.

64. Chivet M, Javalet C, Laulagnier K, Blot B, Hemming FJ, Sadoul R. Exosomes secreted by cortical neurons upon glutamatergic synapse activation specifically interact with neurons. J Extracell Vesicles. 2014;

65. Fais S, O'Driscoll L, Borras FE, Buzas E, Camussi G, Cappello F, et al. Evidence-Based Clinical Use of Nanoscale Extracellular Vesicles in Nanomedicine. ACS Nano. 2016.

66. Shah R, Patel T, Freedman JE. Circulating extracellular vesicles in human disease. N. Engl. J. Med. 2018.

67. Ye W, Tang X, Yang Z, Liu C, Zhang X, Jin J, et al. Plasma-derived exosomes contribute to inflammation via the TLR9-NF-κB pathway in chronic heart failure patients. Mol Immunol. 2017;

68. Martin PJ, Héliot A, Trémolet G, Landkocz Y, Dewaele D, Cazier F, et al. Cellular response and extracellular vesicles characterization of human macrophages exposed to fine atmospheric particulate matter. Environ Pollut. 2019;

69. Stassen FRM, van Eijck PH, Savelkoul PHM, Wouters EFM, Rohde GGU, Briedé JJ, et al. Cell Type- and Exposure-Specific Modulation of CD63/CD81-Positive and Tissue Factor-Positive Extracellular Vesicle Release in response to Respiratory Toxicants. Oxid Med Cell Longev. 2019;

70. Xu Z, Wang N, Xu Y, Hua L, Zhou D, Zheng M, et al. Effects of chronic PM2.5 exposure on pulmonary epithelia: Transcriptome analysis of mRNA-exosomal miRNA interactions. Toxicol Lett. 2019;

71. Bollati V, Angelici L, Rizzo G, Pergoli L, Rota F, Hoxha M, et al. Microvesicle-associated microRNA expression is altered upon particulate matter exposure in healthy workers and in A549 cells. J Appl Toxicol. 2015;

72. Bonzini M, Pergoli L, Cantone L, Hoxha M, Spinazzè A, Del Buono L, et al. Short-term particulate matter exposure induces extracellular vesicle release in overweight subjects. Environ Res. 2017;

73. Emmerechts J, Jacobs L, van Kerckhoven S, Loyen S, Mathieu C, Fierens F, et al. Air pollution-associated procoagulant changes: The role of circulating microvesicles. J Thromb Haemost. 2012;

74. Pergoli L, Cantone L, Favero C, Angelici L, Iodice S, Pinatel E, et al. Extracellular vesicle-packaged miRNA release after short-term exposure to particulate matter is associated with increased coagulation. Part Fibre Toxicol. 2017;

75. Chiarello DI, Salsoso R, Toledo F, Mate A, Vázquez CM, Sobrevia L. Foetoplacental communication via extracellular vesicles in normal pregnancy and preeclampsia. Mol. Aspects Med. 2018.

76. Burnett LA, Nowak RA. Exosomes mediate embryo and maternal interactions at implantation and during pregnancy. Front Biosci - Sch. 2016;

77. Kurian NK, Modi D. Extracellular vesicle mediated embryo-endometrial cross talk during implantation and in pregnancy. J. Assist. Reprod. Genet. 2019.

78. Hemmatzadeh M, Shomali N, Yousefzadeh Y, Mohammadi H, Ghasemzadeh A, Yousefi M. MicroRNAs: Small molecules with a large impact on pre-eclampsia. J. Cell. Physiol. 2020.

79. Vilella F, Moreno-Moya JM, Balaguer N, Grasso A, Herrero M, Martínez S, et al. Hsa-miR-30d, secreted by the human endometrium, is taken up by the pre-implantation embryo and might modify its transcriptome. Dev. 2015;

80. Kaminski V de L, Ellwanger JH, Chies JAB. Extracellular vesicles in host-pathogen interactions and immune regulation — exosomes as emerging actors in the immunological theater of pregnancy. Heliyon. 2019.

81. Mangeney M, Renard M, Schlecht-Louf G, Bouallaga I, Heidmann O, Letzelter C, et al. Placental syncytins: Genetic disjunction between the fusogenic and immunosuppressive activity of retroviral envelope proteins. Proc Natl Acad Sci U S A. 2007;

82. Vargas A, Zhou S, Eťhier-Chiasson M, Flipo D, Lafond J, Gilbert C, et al. Syncytin proteins incorporated in placenta exosomes are important for cell uptake and show variation in abundance in serum exosomes from patients with preeclampsia. FASEB J. 2014;

83. Fisher SJ. Why is placentation abnormal in preeclampsia? Am. J. Obstet. Gynecol. 2015.

84. Salomon C, Sarah Y, Scholz-Romero K, Kobayashi M, Vaswani K, Kvaskoff D, et al. Extravillous trophoblast cells-derived exosomes promote vascular smooth muscle cell migration. Front Pharmacol. 2014;

85. Hadley EE, Sheller-Miller S, Saade G, Salomon C, Mesiano S, Taylor RN, et al. Amnion epithelial cell–derived exosomes induce inflammatory changes in uterine cells. Am J Obstet Gynecol. 2018;

86. Pillay P, Maharaj N, Moodley J, Mackraj I. Placental exosomes and pre-eclampsia: Maternal circulating levels in normal pregnancies and, early and late onset pre-eclamptic pregnancies. Placenta. 2016;

87. Salomon C, Guanzon D, Scholz-Romero K, Longo S, Correa P, Illanes SE, et al. Placental exosomes as early biomarker of preeclampsia: Potential role of exosomalmicrornas across gestation. J Clin Endocrinol Metab. 2017;

88. Levine L, Habertheuer A, Ram C, Korutla L, Schwartz N, Hu RW, et al. Syncytiotrophoblast extracellular microvesicle profiles in maternal circulation for noninvasive diagnosis of preeclampsia. Sci Rep. 2020;

89. Salomon C, Scholz-Romero K, Sarker S, Sweeney E, Kobayashi M, Correa P, et al. Gestational diabetes mellitus is associated with changes in the concentration and bioactivity of placenta-derived exosomes in maternal circulation across gestation. Diabetes. 2016;

90. Miranda J, Paules C, Nair S, Lai A, Palma C, Scholz-Romero K, et al. Placental exosomes profile in maternal and fetal circulation in intrauterine growth restriction - Liquid biopsies to monitoring fetal growth. Placenta. 2018;

91. Rodosthenous RS, Burris HH, Sanders AP, Just AC, Dereix AE, Svensson K, et al. Second trimester extracellular microRNAs in maternal blood and fetal growth: An exploratory study. Epigenetics. 2017;

92. Rawls M, Ellis AK. The microbiome of the nose. Ann. Allergy, Asthma Immunol. 2019.

93. Whelan FJ, Verschoor CP, Stearns JC, Rossi L, Luinstra K, Loeb M, et al. The loss of topography in the microbial communities of the upper respiratory tract in the elderly. Ann Am Thorac Soc. 2014;

94. Wos-Oxley ML, Chaves-Moreno D, Jáuregui R, Oxley APA, Kaspar U, Plumeier I, et al. Exploring the bacterial assemblages along the human nasal passage. Environ Microbiol. 2016;

95. Hibbing ME, Fuqua C, Parsek MR, Peterson SB. Bacterial competition: Surviving and thriving in the microbial jungle. Nat. Rev. Microbiol. 2010.

96. Khan R, Petersen FC, Shekhar S. Commensal bacteria: An emerging player in defense against respiratory pathogens. Front. Immunol. 2019.

97. Petersen C, Round JL. Defining dysbiosis and its influence on host immunity and disease. Cell. Microbiol. 2014.

98. Hoggard M, Waldvogel-Thurlow S, Zoing M, Chang K, Radcliff FJ, Mackenzie BW, et al. Inflammatory endotypes and microbial associations in chronic rhinosinusitis. Front Immunol. 2018;

99. Lu Z. Microbiota research: From history to advances. E3S Web Conf. 2020.

100. http://www.human-microbiome.org/.

101. Fricker AM, Podlesny D, Fricke WF. What is new and relevant for sequencing-based microbiome research? A mini-review. J. Adv. Res. 2019.

102. Franzosa EA, Hsu T, Sirota-Madi A, Shafquat A, Abu-Ali G, Morgan XC, et al. Sequencing and beyond: Integrating molecular “omics” for microbial community profiling. Nat. Rev. Microbiol. 2015.

103. Rideout JR, He Y, Navas-Molina JA, Walters WA, Ursell LK, Gibbons SM, et al. Subsampled open-reference clustering creates consistent, comprehensive OTU definitions and scales to billions of sequences. PeerJ. 2014;

104. Amir A, McDonald D, Navas-Molina JA, Kopylova E, Morton JT, Zech Xu Z, et al. Deblur Rapidly Resolves Single-Nucleotide Community Sequence Patterns. mSystems. 2017;

105. Callahan BJ, McMurdie PJ, Rosen MJ, Han AW, Johnson AJA, Holmes SP. DADA2: High-resolution sample inference from Illumina amplicon data. Nat Methods. 2016;

106. Callahan BJ, McMurdie PJ, Holmes SP. Exact sequence variants should replace operational taxonomic units in marker-gene data analysis. ISME J. 2017;

107. Bolyen E, Rideout JR, Dillon MR, Bokulich NA, Abnet CC, Al-Ghalith GA, et al. Reproducible, interactive, scalable and extensible microbiome data science using QIIME 2. Nat. Biotechnol. 2019.

108. Vandeputte D, Kathagen G, D’Hoe K, Vieira-Silva S, Valles-Colomer M, Sabino J, et al. Quantitative microbiome profiling links gut community variation to microbial load. Nature. 2017;

109. Silibello C, Calori G, Brusasca G, Giudici A, Angelino E, Fossati G, et al. Modelling of PM10 concentrations over Milano urban area using two aerosol modules. Environ Model Softw. 2008;

110. Cantone L.* , Hoxha M. and B V. Characterization of microvesicles using the MACSQuant® Analyzer.

111. Rognes T, Flouri T, Nichols B, Quince C, Mahé F. VSEARCH: A versatile open source tool for metagenomics. PeerJ. 2016;

112. Lee H, Abston E, Zhang D, Rai A, Jin Y. Extracellular vesicle: An emerging mediator of intercellular crosstalk in lung inflammation and injury. Front. Immunol. 2018.

113. Soni S, Wilson MR, O’Dea KP, Yoshida M, Katbeh U, Woods SJ, et al. Alveolar macrophage-derived microvesicles mediate acute lung injury. Thorax. 2016;

114. Moon HG, Cao Y, Yang J, Lee JH, Choi HS, Jin Y. Lung epithelial cell-derived extracellular vesicles activate macrophage-mediated inflammatory responses via ROCK1 pathway. Cell Death Dis. 2015;

115. Benedikter BJ, Wouters EFM, Savelkoul PHM, Rohde GGU, Stassen FRM. Extracellular vesicles released in response to respiratory exposures: implications for chronic disease. J. Toxicol. Environ. Heal. - Part B Crit. Rev. 2018.

116. Chuong EB. The placenta goes viral: Retroviruses control gene expression in pregnancy. PLoS Biol. 2018.

117. Pope CA, Bhatnagar A, McCracken JP, Abplanalp W, Conklin DJ, O’Toole T. Exposure to Fine Particulate Air Pollution Is Associated with Endothelial Injury and Systemic Inflammation. Circ Res. 2016;

118. van den Hooven EH, Pierik FH, de Kluizenaar Y, Hofman A, van Ratingen SW, Zandveld PYJ, et al. Air pollution exposure and markers of placental growth and function: The Generation R Study. Environ Health Perspect. 2012;

119. Breitner S, Peters A, Zareba W, Hampel R, Oakes D, Wiltshire J, et al. Ambient and controlled exposures to particulate air pollution and acute changes in heart rate variability and repolarization. Sci Rep. 2019;

120. Hampel R, Lepeule J, Schneider A, Bottagisi S, Charles MA, Ducimetière P, et al. Short-term impact of ambient air pollution and air temperature on blood pressure among pregnant women. Epidemiology. 2011;

121. Klepac P, Locatelli I, Korošec S, Künzli N, Kukec A. Ambient air pollution and pregnancy outcomes: A comprehensive review and identification of environmental public health challenges. Environ. Res. 2018.

122. Hao J, Zhang F, Chen D, Liu Y, Liao L, Shen C, et al. Association between ambient air pollution exposure and infants small for gestational age in Huangshi, China: a cross-sectional study. Environ Sci Pollut Res. 2019;

RINGRAZIAMENTI

Dedico questa pagina ai ringraziamenti verso coloro che mi hanno seguito durante la durata del progetto di dottorato ed hanno reso la produzione di questa tesi possibile. Ringrazio in primo luogo **TUTTI I MEMBRI del EPIGET LAB** ed in particolare la dott.ssa Simona Iodice per il supporto fornito per le analisi statistiche.

Ringrazio il prof. Nicola Persico e in generale la -'Clinica Mangiagalli' '-Ospedale Maggiore Policlinico per aver permesso l'arruolamento e il monitoraggio dei pazienti coinvolti nel progetto INSIDE.

Ringrazio anche il gruppo di ricerca dell'Università dell'Insubria, in particolare dott. Andrea Cattaneo e dott.ssa Francesca Borghi, per la fase di arruolamento dei pazienti e l'elaborazione dei dati relativi alle concentrazioni di inquinanti.

Ringrazio il dott. Marco Vicenzi e il team del -'Dyspnea Lab' - Ospedale Maggiore Policlinico per i dati raccolti durante le visite cardiologiche.

Infine, il ringraziamento più grande va alla mia tutor prof.ssa Cecilia Angela Pesatori e alla prof.ssa Valentina Bollati, per il sostegno non solo per questa tesi, ma in ogni progetto in cui sono stato coinvolto durante il mio dottorato.